CAPITAL UNIVERSITY OF SCIENCE AND TECHNOLOGY, ISLAMABAD

Finite Element Analysis of Heat Transfer in a Micromagnetorotation Flow Within Micropolar Continuum

by

Irum Zaffar

A thesis submitted in partial fulfillment for the degree of Master of Philosophy

in the

Faculty of Computing
Department of Mathematics

2025

This thesis is dedicated to my beloved and cherish mom who always keeps me motivated and positive whenever I got fed up with this and wanted to quit, to my father, Muhammad Zaffar Iqbal for letting me reach at this level and finally to Dr. Muhammad Sabeel Khan for his patience throughout my work.

CERTIFICATE OF APPROVAL

Finite Element Analysis of Heat Transfer in a Micromagnetorotation Flow Within Micropolar Continuum

by

Irum Zaffar

(Registration No: MMT231009)

THESIS EXAMINING COMMITTEE

S. No.	Examiner	Name	Organization
(a)	External Examiner	Dr. Azad Hussain	University of Gujrat, Gujrat
(b)	Internal Examiner	Dr. Muhammad Sagheer	CUST, Islamabad
(c)	Supervisor	Dr. Muhammad Sabeel Khan	CUST, Islamabad

Dr. Muhammad Sabeel Khan
Thesis Supervisor
March, 2025

Dr. Muhammad Sagheer
Head
Dept. of Mathematics
March, 2025

Dr. Muhammad Abdul Qadir
Dean
Faculty of Computing
March, 2025

Author's Declaration

I, **Irum Zaffar** hereby state that my MPhil thesis titled "**Finite Element Analysis of Heat Transfer in a Micromagnetorotation Flow Within Micropolar Continuum**" is my own work and has not been submitted previously by me for taking any degree from Capital University of Science and Technology, Islamabad or anywhere else in the country/abroad.

At any time if my statement is found to be incorrect even after my graduation, the University has the right to withdraw my MPhil Degree.

(Irum Zaffar)

Registration No: MMT231009

Plagiarism Undertaking

I solemnly declare that research work presented in this thesis titled "**Finite Element Analysis of Heat Transfer in a Micromagnetorotation Flow Within Micropolar Continuum**" is solely my research work with no significant contribution from any other person. Small contribution/help wherever taken has been duly acknowledged and that complete thesis has been written by me.

I understand the zero tolerance policy of the HEC and Capital University of Science and Technology towards plagiarism. Therefore, I as an author of the above titled thesis declare that no portion of my thesis has been plagiarized and any material used as reference is properly referred/cited.

I undertake that if I am found guilty of any formal plagiarism in the above titled thesis even after award of MPhil Degree, the University reserves the right to withdraw/revoke my MPhil degree and that HEC and the University have the right to publish my name on the HEC/University website on which names of students are placed who submitted plagiarized work.

(Irum Zaffar)

Registration No: MMT231009

Acknowledgement

The universe was created in the name of ALLAH (SWT), the most merciful and benevolent being, who also gave humanity the intelligence and wisdom to discover its secrets. I want to sincerely thank ALLAH (SWT) and show my supervisor, Dr. Muhammad Sabeel Khan, my utmost admiration for his enthusiastic attention, willingness to supervise, excellent leadership, and inspiration during this inquiry. I was able to format this thesis thanks to his verbal and textual criticism. I am incredibly appreciative to all of my teachers for their support and emphasis on aiming for excellence in mathematics instruction. For giving me such a conducive setting for this research, I would like to thank CUST. I must sincerely thank my parents and my entire family, especially my cherished Uncle Liaquat Ali Khan and Aunties Farah and Musarat, for their unwavering support and unceasing encouragement during my years of education as well as during the research and writing of this thesis. Lastly, I would want to thank my friends for supporting me during my MPhil research. For their insightful discussions on this research, I am appreciative of my fellow CUST researchers. It has been a pleasure dealing with them in a welcoming atmosphere.

(Irum Zaffar)

Registration No: MMT231009

Abstract

This thesis presents a thermal flow model's finite element analysis while taking micro-magnetorotation (MMR) effects into account. In order to determine how MMR affects the thermal and hydrodynamics of the flow system under consideration, we examine a heat transfer model in micropolar continuum. The impact of MMR is then included to this model. This allows to examine how MMR affects the flow under consideration's thermal, velocity, and microrotational velocity fields. For simplicity, the flow is taken into account in a square cavity. Geometry's description and related boundary conditions are given. The partial differential equations (PDEs) provide the expanded model that governs the flow dynamics within the cavity. The proposed model based on PDEs is non-dimensionalized for the analysis. A weak formulation of the related flow problem is then constructed using this non-dimensinalized system. The open source code FreeFEM++, which is based on the finite element method, is used to implement the developed weak formulation. The solution to the cavity flow problem under various material parameter settings is calculated by numerical simulations. For different physical parameters, the temperature, velocity, and microrotatinal velocity field variables are calculated and presented both with and without the MMR effect.

Contents

List of Figures

Abbreviations

DFP	Darcy Forchheimer Porous
FEM	Finite Element Method
GFEM	Galerkin Finite Element Method
HD	Hydrodynamic
MHD	Microhydrodynamic
MMR	Micromagnetorotation
MP	Micropolar
MR	Microrotation

Symbols

U	x-component of velocity
x,y	Cartesian coordinates
w	Angular Velocity
$\frac{\partial}{\partial x}$	Partial derivative w.r.t coordinate x
Pr	Prandtl number
Re	Reynolds number
Rm	Magnetic Reynolds number
N	Coupling number
Ha	Hartmann number
Br	Brinkmann number
h	Magnetization Parameter
ht	Relaxed Magnetization Factor
τ	Relaxation Time of Magnetization
a	Length of domain
α	Micropolar Magnetic Constant
ξ	Magnetic Ratio Parameter
M_p	Magnetic Parameter
μ_0	Magnetic Permeability
σ	Electrical Conductivity
M	Magnetization Vector
M_0	Magnetization Strength
B	Magnetic Induction Vector
j	Current Density
$\bar{H}$	Magnetiude of Magnetic Field Vector

∇	Gradient Vector
μ	Microrotational units of Viscosity
k	Microrotational units of Viscosity
μ_m	Magnetic viscosity
ω_1	Microrotational Velocity in x-direction
ω_2	Microrotational Velocity in y-direction
Ω	Domain
θ	Temperature
ρ	Density of Fluid
P	Pressure
u	Micropolar Fluid velocity vector
j^*	Microgyration Constant
K_f	Thermal Conductivity
C_P	Specific Heat at Constant Pressure and Electrucal Conductivity
D	Strain Rate Tensor

Chapter 1

Introduction and Literature Survey

In a micropolar flow, the fluids have microstructure. In such flows, the fluid particles have rotating degree of freedom separate from their translational movements, just as viscous fluids. The non-symmetric nature of the stresses in micropolar flow theory necessitates the use of an extra balance law. For example, the dynamical account of the conservation of angular momentum. The importance of considering additional momentum balance in mechanical description is highlighted through its practical applications. These applications include magnetic refrigeration (enhanced heat transfer efficiency) [1], heat exchangers (improved designs and optimization) [2], magnetic resonance imaging (MRI) (efficient cooling system) [3], magnetic storage devices (thermal management and heat dissipation) [4], sprintonics (controlled heat transfer and spin-polarized currents) [5], magnetic fluids (heat transfer and fluid flow optimization) [6], biomedical applications (hyperthermia treatment and magnetic particle dynamics) [7], aerospace engineering (thermal protection systems and heat shields) [8].

The continuum description of MP theory is emerged in early 1960s. Lev Landau (1908-1968) is considered to be the first researcher who introduce the concept of micromagnetism and gave the idea of magnetic domains in the 1930s. William Fuller Brown Jr. further developed the concept of micromagnetism and magnetic domains, building upon Lav Ladau's, as referenced in [9] .

This article is considered a seminal work in the field of micromagnetism. Micromagnetorotation describes the local, rotational movement of the microscopic components within a fluid when subjected to a magnetic field. According to micropolar theory, the internal particles of fluids with a wide range of microstructures may rotate independently of their linear velocity [10, 11].

Aslani et al. [12] recently study the impact of micromagnetorotation (MMR) effect on micropolar magnethydrodynamic flow that has potential applications in various fields, including biomedical engineering, biomechanics, chemical engineering, geophysics, material sciences.

Numerous people have studied micropolar flows in the finite element description in the literature. In term of the problem's geometry and physics, the majority of these researches are in limiting instance. Many researches, for example, focus on the one-dimensional boundary layer flow phenomena, which occurs when similarity transformations are applied to a two-dimensional and occasionally three-dimensional model, reducing it to one-dimensional. A chemically reactive MP rotating liquid's boundary layer analysis across a flat plate was examined by Sheri et al. [13]. They used a variational finite element approach to solve the governing flow dynamic equation in order to examine the impacts of Hall power and sticky dispersion. Profiles of state fields, skin friction, and pair stress were displayed in relation to physical parametric changes. Khan et al. [14] studied that under the influence of an external magnetic field, the flow is regarded as laminar and incompressible. Haque [15] examines the heat and mass transfer in a magneto micropolar fluid flow along a semi-infinite vertical plate with an induced magnetic field. Khan and Hameed [16] examined heat transfer through a channel and electrically induced magnetic incompressible flow using micropolar continuum framework.

Pattnaik, Mishra and Panda [17] studied the use of magnetic field interaction to maximize the heat transfer rate for micropolar fluid flow across a shrinking surface. Bejawada and Nandeppanavar [18] investigate an analysis for this study of magnetohydradynamics, heat transfer flow of the micropolar fluid over a vertical porous moving plate in the existance of the radiation effect. Gupta et al. [19] solved numerically the continuous mixed convection magnetohydrodynamic flow of an electrically conducting micropolar fluid across a porous shrinking sheet. Shamsuddin and Ibrahim [20] investigated the Casson fluid's electro-magnetohydradynamic flow through parallel plates using a micropolar description. Using a finite element method in a one-dimensional context, the controlling flow equations for temperature, velocity, and MR profiles are resolved. They discovered that the heat transport in nanofluids are greatly impacted by both thermodiffusion and brown's behaviour of particles. Takhar et al. [21] investigated the continuous symmetrical circulation between the transparent plates and the energy transmission of a dense MP liquid. They used the finite element approach to resolve the controlling differential system in 1-D, and by varying values of the micropolar parameter, along with other characteristics related to skin-friction and the coupling stress coefficient, they also looked at the temperature, velocity, and MR profiles. Studies in micropolar theory are taken in numerous geometrical and physical contexts, and other numerical techniques have also been employed. For example, Papausky et al.[22] examined how micropolar fluids move laminarly through microchannels. For a good review, the reader can find the paper by Kambli and Dey [23] for a thorough examination of the most recent advancements in the analysis of heat transfer through micro-channel flow. They displayed different micro channels with various fluids to illustrate how thermal management is used in engineering across numerous industrial sectors. Characteristics of heat transport in a square mini-channel, which are frequently utilized in power batteries and tiny electronic devices, were examined by Feng et al. [24]. Amiri and Mikielewicz [25] have studied flow across chain micro-channels in a 3D environment using a classical continuum approach. Single-sided heating in a rectangular channel is important for space scientific applications. Ghosh, Sarkar and Sekhar [26] investigated magnetohydrodynamic channel flow in two dimensions and in a classical continuum framework using the open source code OpenFOAM. In a joint experiment, along Mudawar et al. [27], researchers from Purdue University's boiling and two-phase flow laboratory and National Aeronautics and Space Administration Glenn research centre, examined heat transmission and microgravity flow. They gave streamwise temperature and thermal coefficient profiles, noted that a few thermodynamical non-equilibrium states in a channel. Murthy, Sai and Bahali [28] measured the micro-rotation velocity and studied the continuous flow of micropolar fluid over a rectangular cable with suction while following a transverse magnetic field. Using a porous medium and a constant pressure gradient, the effect of magnetic fields on the flow between two Newtonian micropolar fluid layers was investigated by Kumar et al. [29]. Borrelli, Giantesio and

Patria [30], uses the Oberbeck-Boussinesq approximation to investigate the effects of temperature and magnetic field on the steady mixed convection in the fully developed flow of a micrpolar fluid filling a vertical channel. The two limits are maintained at either differing or equal temperature and are regarded as isothermal. An analytical results are obtained for the temperature, the individual magnetic field, the velocity and microrotation. Khan and Hackl [31] talked about the relaxed energy model of the micropolar continuum. They examined the material's underyling microstructures and took into an account the partcicles' counterrotations. The influences of Prandtl, Reynolds and Rayleigh's numbers on temperature, streamlines, and velocity profiles were further studied by Ignor et al. [32], who proposed the model for connective heat transfer in MP flow in a channel. Dinarvand, Saber and Abulhasansari [33] examined heat transfer in MP fluid via a cone in spinning while taking ohmic heating effect and Hall current into account. They examined the impact of different material constants and performed an analytical analysis of the power change in surface temperature. Using a finite element formulation, Asadi, Javaherdeh and Ramezani [34] showed a MP blood flow in circular channel and figured out that the length-scale and MP viscosity have a significant impact on the flow's properties. In a micropolar hybrid nano-fluids, Khan and Kaneez [35] searched computational solution of heat flow by employing a Petrov-Galerkin approach based on the finite element method. They investigated the effects of physical parameters on the thermal boundary layer, including the Eckert number, magnetic parameter, Cosserat rotational factor, and nanoparticle concentration variables. Only a simplified geometrical explanation of the event under consideration is provided in the previously discussed literature and a classical framework was used to discuss the problem's physics. In present contribution, we extend the work of Khan and Hameed [16] with the effect of MMR. In this regard, theory of magnetization is taken into account. Furthermore, the current contribution considers a model with two-dimensional geometry in a non-classical continuum environment and introduces a numerical method that is more effective than standard finite elements based on Galerkin approach. Because of the symmetric boundary conditions, the problem's geometry has been studied in two dimensions.

In comparison to the conventional Galerkin technique, the characteristic-Galerkin approach, on which the method is based, enables the management of longer time-steps and higher resolution of the underlying physics. FreeFEM++ is a new multiphysics code that is used to present the model problem. The analytical solution in a simplified micropolar flow model scenario is used to validate the acquired results.

This analysis not only highlights the open source code's potential utility in mass and heat transport analysis but also highlights its advantages in relevant technical applications as well. It is important to note that because of their numerous uses in industrial solutions, the results displayed are of significant technological value.

1.1 Thesis Contribution

This thesis analyzes a thermal flow model using finite element analysis and micromagnetorotation effects. It examines the impact of MMR on the thermal and hydrodynamics of a flow system, focusing on a square cavity flow problem. The model is first presented using set of partial differential equations incorporated with the impact of MMR. The PDEs model that is presented in this thesis, is first non-dimensionalized using a set of transformations and then a weak variational form of it is calculated. This gives the basis to the finite element setting and this weak form of the model is then implemented in the open source code FreeFEM++. The implemented model is used to compute the solution for varying physical parameters in the absence and presence of MMR effects. Numerical simulations are used to calculate the cavity flow problem under different material parameters. Flow dynamics and thermal behavior is anlayzed within the cavity using numerical analysis and the implemented code. Results are presented and discussed in detail with concluding some interesting findings.

- The temperature increases significantly in the presence of MMR compared to the absence of MMR effect.
- The temperature in the medium increases significantly with increasing material parameter α_1 due to the MMR effect.
- It is seen that in the presence of MMR, the temperature within the medium increases with increasing values of the parameter Br.

1.2 Objectives

The objectives of this study are described below.

- To propose a PDE based mathematical model to analyze the thermal behavior within a square cavity with MMR effects.
- To develop the finite element model based on the weak formulation of the presented PDE model.
- To implement the developed weak form of the proposed thermal model in the open source code FreeFEM++.
- To simulate the flow dynamics in a square cavity in the presence of MMR effects
- To compute the effect of MMR on the thermal, velocity and micromagnetorotation field variables within the square cavity.

1.3 Thesis Layout

This thesis is further consists of the following chapters:

- **Chapter 2** illustrates the fundamentals of fluid dynamics. The fundamental concepts and laws, fluid motion controlling laws, types of fluid flow like Newtonian and non-Newtonian flow, laminar, transitional and turbulent flow, one, two and three dimensional flow, compressible and incompressible flow, steady and unsteady flow, uniform and non-uniform flow, viscosity and its types, shearing, shear stress and governing equations have been briefly discussed and illustrated.

  Introduction to FreeFEM++ has been discussed in detail. Its applications and advantages are equally crucial to be studied. Stress Rate Tensor is also defined.

- **Chapter 3** describes the review of [16]. In this paper, a research is carried to examine heat transfer and electrically generated magnetic incompressible flow along a channel using the micropolar continuum framework.

By computing the numerical solutions through finite element method, it has been noted that raising the micropolar coupling constant causes the medium's maximum temperature to move from the domain's center towards its boundaries.

- **Chapter 4** presents the mathematical model of finite element analysis of heat transfer in a MMR flow within the framework of micropolar continuum. This chapter investigates the numerical simulations of heat transfer through a square cavity channel with the effect of MMR. In the absence of body force and couples, the governing system of dynamical equation is defined. Non-Dimensional form is obtained from component form using different transformational variables. The weak form is computed and variational problem is imbedded in FREEFEm++ language. In order to verify that the problem was correctly implemented and that the numerical results were obtained, a reduced micropolar magnetohydrodynamic model is considered. Numerical solutions are computed through finite element method.

- **Chapter 5** in this chapter, we present results computed using the finite element method. The results are calculated for varying different material parameters and are discussed in detail. FreeFEM++ code is developed to calculate the solution numerically.

- **Chapter 6** this chapter comprises of conclusion and discussion about the importance of this thesis in future.

References related to present work are listed in Bibliography.

Chapter 2

Fundamental Concepts of Fluid Mechanics

We will discuss the basic concepts, definition and governing laws related to fluid dynamics. Dimensional quantities will also be considered here which seems to be helpful in the subsequent chapters.

2.1 Basic Definitions

2.1.1 Physical Properties of the Fluid

2.1.1.1 Mass Density or Density

Density of the fluid is defined as the ratio between mass of the fluid and volume of the fluid. It is denoted by ρ. The unit of mass density is Kg per cubic metre, i.e; Kg/m^3. Mathematically, it is written as

$$\rho = \frac{\text{Mass of fluid}}{\text{Volume of fluid}}.$$

The value of density of water is $1gm/cm^3$ or $1000Kg/m^3$.

2.1.1.2 Pressure

Pressure is the amount of force applied perpendicular to the surface of an object per unit area.

$$P = \frac{F}{A}.$$

F=Force,
A=Area on which force acts.

2.2 Dimensionless Parameters

Following are the dimensionless numbers that will appear in our discussion.

2.2.1 Reynolds Number

The Reynolds number is a dimensionless quantity that helps predict fluid flow patterns in different situations. It is calculated by comparing the ratio of inertial forces to viscous forces within a fluid. Its formula is

$$R_e = \frac{LV}{\nu},$$

where,

L is the characteristic length of the domain,

V is the fluid velocity,

ν is the fluid viscosity

2.2.2 Hartmann Number

The Hartmann number is a dimensionless quantity that characterizes the interaction between electromagnetic forces and viscous forces in electrically conducting fluids.It is particularly important in the field of magnetohydrodynamics (MHD). It is defined as the ratio of the electromagnetic force to the viscous force. Its formula is

$$Ha = Bl\sqrt{\frac{\sigma}{\nu\rho}},$$

where,
B is the magnetic flux density,
l is the characteristic length,
ν is the kinematic viscosity,
ρ is the mass density,
σ is the electric conductivity.

2.2.3 Reynolds Magnetic Number

The magnetic Reynolds number is a dimensionless quatity that characterizes the relative importance of advection (transport by fluid motion) and diffusion of the magnetic field in a conducting fluid. Its formula is

$$Rm = \mu\sigma VL,$$

where,
μ is the magnetic permeability,
σ is the electrical conductivity of the fluid,
V is the characteristic velocity of the fluid flow,
L is the characteristic length scale of the fluid flow.

2.2.4 Brinkman

The Brinkman number is a dimensionless number that represents the ratio of heat generated by viscous dissipation to heat conducted away from the system.

$$Br = \frac{\mu U^2}{k(Tw - T_0)},$$

where,

μ is the dynamic viscosity of the fluid,

U is the flow velocity of the fluid,

k is the thermal conductivity of the fluid,

Tw is the wall temperature,

T_0 is the bulk fluid temperature.

2.2.5 Coupling Number

The coupling number is a dimensionless quantity that characterizes the strength of the coupling between different physical phenomena. The coupling number is a dimensionless quantity in micropolar elasticity that characterizes the degree of micropolarity exhibited by a material. It provides valueable insights into the material's behavior and is essential for accurate modeling and simulation of materials with microstructure.

2.3 Types of Fluid Flow

2.3.1 Steady and Unsteady Flow

- **Steady Flow**

  The fluid flow is said to be steady if:

  1. Velocity remains constant at every point.
  2. Pressure remains constant at every point.
  3. Density remains constant at every point.

  Mathematically, it can be written as:

$$\frac{\partial V}{\partial t} = 0,$$

$$\frac{\partial P}{\partial t} = 0,$$

$$\frac{\partial \rho}{\partial t} = 0.$$

For Example: Flow through a nozzle.

- **Unsteady Flow**

  The fluid flow is said to be unsteady if:

  1. Velocity changes at every point with time.
  2. Pressure changes at every point with time.
  3. Density changes at every point with time.

  Mathematically it can be written as:

$$\frac{\partial V}{\partial t} \neq 0,$$

$$\frac{\partial P}{\partial t} \neq 0,$$

$$\frac{\partial \rho}{\partial t} \neq 0.$$

  For Example: Ocean waves and tides.

2.3.2 Uniform and Non-Uniform Flow

2.3.2.1 Uniform Flow

Such type of fluid flow where characteristics of flow remains constant along the flow path is known as uniform flow. It means all the properties of the fluid such as velocity, pressure and depth do not vary from point to point along the flow. i.e; constant velocity, constant cross-sectional area and steady flow. For Example: Water flowing in a long, straight pipe with a constant diameter.

2.3.2.2 Non-Uniform Flow

Such type of fluid flow where characteristics of the flow vary along the path is known as non-uniform flow. This could be happen when the size or shape of the flow channel is changed, obstructions in the flow or other factors. For Example: Water flowing in a pipe with a bend or change in diameter.

2.3.3 Newtonian and Non-Newtonian Flow

2.3.3.1 Newtonian Flow

Any fluid whose viscosity remains constant when the amount of shear is applied at a constant temperature is called Newtonian flow.

For Example: Water, air, honey (at high temperature).

2.3.3.2 Non-Newtonian Flow

Non-Newtonian flows are opposite of the Newtonian flows i.e; on applying shear, the viscosity of non-Newtonian flow changes, depending on the fluid.

For Example: Hair gel, egg white.

2.3.4 Laminar Flow, Turbulent Flow and Transition Flow

2.3.4.1 Laminar Flow

The fluid flows in parallel layers or streams, with no random motions or mixing between layers with less Reynolds number ($Re < 2000$). Such type of flow is known as Laminar Flow.

For Example: Water flow through a small pipe, air flow through a narrow tube.

2.3.4.2 Turbulent Flow

The fluid flows in irregular, random motions, resulting in mixing between different fluid layers with high Reynolds number ($Re > 4000$). Such type of flow is known as Turbulent Flow.

For Example: Water flow through a rough pipe, stormy weather with strong winds.

2.3.4.3 Transitional Flow

The fluid flow that exhibits the characteristics of both turbulent and laminar flows, occuring when the flow is in the way of transtioning from laminar to turbulent or turbulent to laminar flow. The Reynolds number is typically in the range of $(2000 - 4000)$.

For Example: Flow in pipe, boundary layer of an airfoil.

2.3.5 One,Two and Three Dimensional Flow

2.3.5.1 One Dimensional Flow

Such type of flow that have only one direction is known as one dimensional flow.

For Example: Flow through a pipe.

2.3.5.2 Two Dimensional Flow

Such type of flow that have two directions is known as two dimensional flow.

For Example: Flow over a flate plate, flow around a cylinder.

2.3.5.3 Three Dimensional Flow

Such type of flow that have three directions is known as three dimensional flow. For Example: Flow in an ocean current.

2.3.6 Compressible and Incompressible Flow

2.3.6.1 Compressible Flow

Such type of flow in which density of fluid changes considerably (being affected to an important degree) is known as Compressible flow.

For Example: Airflow around an airplane: Air density changes noticeably at high temperature and makes it a Compressible flow.

2.3.6.2 Incompressible Flow

Incompressible flow is a form of flow when the fluid's density stays roughly constant. For Example: Oceans flow is considered as example of incompressible flow as the density changes are relatively small.

2.4 Viscosity and Its Types

- **Viscosity**

Fluid's resistance to flow or deformation is measured by its viscosity. It depends on the internal fluid layers as they relative to each other. Viscosity is related to the "Thickness" of a fluid. e.g; syrup has a higher viscosity than water.

Types of Viscosity

We can measure viscosity by two methods. The two types of viscosity are:

1. **Dynamic Viscosity** The resistance of a fluid to shear stress, a force that causes a fluid to deform by sliding along a surface is measured by its dynamic viscosity. It is a basic characteristic of fluids that characterizes their "thickness" or flow resistance.

   Stated differently, dynamic viscosity quantifies the degree to which a fluid resists changes in flow rate or form in response to an applied force.

   A fluid seems "thicker" and has greater flow resistance when its dynamic viscosity is higher.

$$\text{Dynamic Viscosity} = \frac{\text{Shearing Stress}}{\text{Shearing Rate Change}}$$

2. **Kinetic Viscosity**

The measurement of a fluid's resistance to flow while subjected to gravity is called kinematic viscosity. It is defined as the fluid's density divided by its dynamic viscosity.

$$\text{Kinematic Viscosity} = \frac{\text{Absolute Viscosity}}{\text{Density of Liquid}}.$$

- **Shearing**

In flows, shearing is the deformation of a fluid brought on by an outside force, usually a fluid velocity gradient. The fluid's shape changes as a result of this deformation, producing shear stress and shear rate.

- **Shear Stress**

Shear stress is defined as unit area amount of force acting on the fluid parallel to a very small element of the surface. It is a measure of the force of friction of fluid from a fluid acting on a body in the path of that fluid. Mathematically, it can be written as:

$$\text{Shear stress} = \frac{\text{Shear Force}}{\text{Cross Sectional Area}} = \frac{F}{A}.$$

2.5 Fundamental Laws

2.5.1 Governing Equations

Such a fundamental mathematical equation that describes the behaviour of a physical system or process is known as governing equation.

For Example:

1. Fluid Dynamics:-
   - Continuity equation(Mass Conservation)

- Navier-Stoke's equation (Momentum conservation)

2. Heat Transfer:-

- Heat Diffusion Equation

3. Electromagnetism:-

- Maxwell's equation: Governing the behaviour of electric and magnetic field.

4. Structural Mechanics:-

- Hooke's Law and Elasticity equation.

2.5.2 Conservation of Mass: the Continuity Equation

- During any physical or chemical process, mass can neither be created nor destroyed in a closed system is known as Law of conservation of Mass.

  In the fluid dynamics, mathematically this principal can be written through continuity equation, which assures that flow of mass in fluid remains constant. The continuity equation is obtained from the conservation of mass.
  It states

$$\frac{\partial \rho}{\partial t} + \nabla \cdot (\rho \mathbf{v}) = 0,$$

  where,

  ρ=Fluid density,

  $\mathbf{V}$=Velocity vector,

  $\nabla \cdot (\rho \mathbf{v})$=Mass Flux's Divergence,

  $\frac{\partial \rho}{\partial t}$=Rate of change of density w.r.t time.

  For incompressible flow, equation of continuity simplifies to:

$$\nabla \cdot \mathbf{v} = 0.$$

  whereas,

ρ =constant,

This implies that in incompressible flow the rate of volume flow is conserved.

2.5.3 Conservation of Energy

In mechanics, we state the Law of conservation of energy as: If system is isolated and no non-conservative forces (i.e; friction or air resistance) act on it then total mechanical energy of the system remains constant. Mathematically, it is equal to the sum of kinetic energy and potential energy.

$$E_T = E_k + E_p.$$

In Conservative System

$$E_k + E_p = \textbf{Constant}.$$

- **Components of Mechanical Energy**

1. Kinetic Energy:

$$E_K = \frac{1}{2}mv^2,$$

   where,

   - m=mass of the object,
   - v=velocity of the object.

2. Potential Energy (e. g; gravitational):

$$E_p = mgh,$$

where,

- m=mass of the object,

- g=acceleration due to gravity,
- h=height above the reference point.

Example

For a free-falling body (ignoring air resistance):

- At the hightest point: E_p is maximum and $E_K = 0$,
- Just before impact: E_k is maximum and $E_p = 0$.

Throughout the motion:

$$E_T = \frac{1}{2}mv^2 + mgh = \text{Constant}.$$

2.5.4 Conservation of Momentum

According to the Newtons's second law of motion also known as the principle of conservation of linear momentum, if the internal forces are governed by Newton's third law of motion, the rate of time at which the linear momentum of a given set of partciles changes is equal to the vector sum of all external forces acting on the set's particles.

The formula for Newton's second Law is

$$\frac{\partial \rho v}{\partial t} + \nabla \cdot (\rho v \phi \ v) = \nabla \cdot \sigma + \rho f,$$

where,

ϕ=Tensor(product of two vectors),

σ=Cauchy stress tensor ($\frac{N}{m^2}$),

f=body force vector (measured by per unit mass and normally taken to be the gravity vector).

Equation explains the motion of continuous medium, and is also known as Navier's equation in fluid mechanics.

2.5.5 Navier-Stokes Equation

In fluid mechanics, the equation that expresses the fluid's motion by describing the conservation of momentum, combined with the effect of viscosity is known as Navier-Stokes Equation.

The behaviour of both incompressible and compressible fluid flows is governed by these equations which are fundamental set of partial differential equations.

- General Form of the Navier-Stokes Equations:

$$\rho\Big(\frac{\partial v}{\partial t} + (v \cdot \nabla)v\Big) = -\nabla P + \mu\nabla^2 v + f$$

where

- ρ=fluid density,
- v=velocity vector of the fluid,
- t=time,
- p=pressure,
- μ=dynamic viscosity,
- $\nabla^2 v$=viscous diffusion term,
- f=external body force per unit volume.

2.6 Finite Element Method

The finite element method (FEM) is a popular method for numerically solving differential equations arising in engineering and mathematical modeling, include structural analysis, heat transfer, fluid flow, mass transport, and electromagnetic potential.

- Divide the whole domain into number of sub-domains, with each subdomain represented by a set of element equations to the original problem.
- Actual problem is expressed by assembly of element equations for each subdomain and then all assembled element equations are recombined within the global system of equations for final computations.

2.6.1 Key Steps in FEM

1. **Discretization of the Domain:**
   - The problem domain is divided into small elements (e.g., triangles, quadrilaterals in 2D, tetrahedrons, or hexahedrons in 3D).
2. **Selection of Interpolation (Shape) Functions:**
   - These functions approximate the unknown variable (e.g., displacement, temperature) within each element.
3. **Derivation of Element Equations:**
   - Using governing equations (such as equilibrium equations in structural mechanics or heat conduction equations), an elemental stiffness matrix is formulated.
4. **Assembly of the Global System:**
   - Individual element equations are assembled into a large system of algebraic equations.
5. **Applications of Boundary Conditions:**
   - Constraints (such as fixed supports or loads) are applied.
6. **Solution of the System of Equations:**
   - The resulting system is solved using numerical methods like Gaussian elimination or iterative solvers.
7. **Post-processing:**

- Results such as stresses, deformations, or temperature distributions are interpreted.

2.6.2 Advantages of FEM

- Can handle complex geometries and boundary conditions.
- Applicable to a wide range of engineering problems.
- Provides approximate but accurate solutions.
- Well-suited for computer implementation and automation.

2.6.3 Applications of FEM

- Structural Analysis: Used to determine stresses, strains, and deformations in structures (e.g., bridges, buildings, automotive frames).
- Heat Transfer: Solves conduction, convection, and radiation problems.
- Fluid Dynamics (CFD): Used for flow analysis in pipes, aircraft aerodynamics, and biomedical simulations.
- Electromagnetic Field Analysis: Applied in designing electrical machines and antennas.

2.7 FreeFEM++

2.7.1 Introduction to FreeFEM++

FreeFEM++ is an open-source software for solving partial differential equations (PDEs) using the Finite Element Method (FEM). It provides a high-level scripting language that makes it easy to define complex problems and perform simulations in 2D and 3D.

2.7.2 Solver

- Variational formulation is obtained through the application of variational calculus.
- Obtained weak formulation of the problem is implemented through the finite element solver FreeFem++.

- Is developed at the Sorbonne University in Paris, France.
- The developing team is lead by Prof. Frédéric Hecht.
- FreeFEM++ is a high level multiphysics solver which is integrated with builtin pre- and post-processing utilities.
- Used to solve PDEs through FEM.

2.7.3 Basic Workflow In FreeFEM++

- Define the mesh.
- Specify the finite element space.
- Define the governing equation (weak form).
- Set boundary conditions.
- Solve the system.
- Post-process results (visualization, exporting data, etc.).

2.8 Stress Rate Tensor

The stress rate tensor describes how the stress tensor evolves over time in a deforming material. It is crucial in continuum mechanics, particularly for modeling viscoelasticity, plasticity, and finite deformations.

- Material (Lagrangian) Time Derivative

$$\dot{\sigma} = \frac{D\sigma}{Dt}$$

This is the time derivative which follows the motion of the material. This is the time derivative following the motion of the material (material derivative).

2.8.1 Applications

- Elastic-plastic deformation in metal forming
- Soft tissue mechanics, or biomechanics
- Geomechanics (modeling of rocks and soil)
- Simulations of elasticity and viscoelasticity in structural engineering

2.9 Darcy Forchheimer Porous Flow

A Darcy Forchheimer flow is a fluid flow pattern across porous surfaces where both Darcy's law and Forchheimer's quadratic resistance law apply simultaneously.

2.9.1 Darcy Law, Forchheimer Law, Porous Medium

- **Darcy Law**: A basic equation known as Darcy's Law explains how a fluid moves through a porous material. Although it has uses in other domains, like as petroleum engineering, it is most frequently employed to comprehend groundwater flow, or the movement of water through the earth.

$$v = \frac{-k}{\mu}\nabla p \tag{2.1}$$

where

- v=Velocity Vector,
- k=Permeability of the Porous Medium,
- μ=Dynamic viscosity of the fluid,
- ∇p=Pressure gradient.

- **Forcheimer Law**:

  Forchheimer's Law expands Darcy's Law by integrating inertial effects for high-velocity fluid flow through a porous material.

  It is appropriate for moderate to high flow rates where Darcy's Law alone is inadequate since it takes into account both viscous (Darcy) and inertial (Forchheimer) resistance.

$$-\nabla p = \frac{\mu}{k}u + \rho\beta u^2 \tag{2.2}$$

where

- P = Pressure [Pa],
- u = Fluid velocity (Darcy velocity) [m/s],
- μ = Dynamic viscosity [Pa·s],
- K = Permeability of the porous medium [m^2],
- ρ = Fluid density [kg/m^3],
- β = Forchheimer coefficient (empirical, depends on medium properties),
- $\frac{\mu}{k}u$ shows viscous resistance (linear term, Darcy Law),
- $\rho\beta u^2$ shows inertial resistance (non-linear term, Forchheimer correction).

- **Porous Medium**:

  A substance with interconnected pores (voids) that allow fluid to pass through is called a porous medium. It is frequently found in biology (biological tissues), engineering (filters, catalysts, and foams), and geology (soil, rock formations).

- **Porous Flow**:

  This describes how a fluid passes through a porous material. It explains the movement of the fluid through the linked pores.

  One of the fundamental ideas guiding porous flow is Darcy's Law, which we covered previously.

Consider it this way:

When water is poured into a porous substance, such as a sponge, it forms porous flow as the water passes through the tiny holes.

2.10 Micromagnetorotation

Micromagnetorotation is the term used to describe how magnetization affects magnetohydrodynamic micropolar flow in fluid mechanics.

- **Key Concepts**

1. **Magnetohydrodynamic**

   The study of interaction between electrically conducting fluids(plasma or metals in liquid form) and magnetic fields is known as Magnetohydrodynamic.

2. **Micropolar Fluids**

   These fluids are microstructured, which means they include small, rotating, hard particles.

   The fluid particles of Newtonian fluids, on the other hand, are thought to be points devoid of interior structure.

   Ferrofluids, blood, and some polymer solutions are examples of micropolar fluids.

3. **Magnetization**

   A substance may get magnetized, that is, its individual atoms may develop a magnetic moment when exposed to a magnetic field.

2.10.1 Importance of MMR in the Present Context

To accurately model and predict the behavior of micropolar fluids in a variety of applications, it is essential to understand MMR, which can have a significant impact on the fluid's velocity profile, flow stability, and internal heat transfer, among other aspects of the fluid's behavior in magnetic fields.Like

1. **Blood Flow:**Understanding MMR can aid in the study of blood flow in the presence of magnetic fields, which has applications in medical treatments such as magnetic medication targeting, since blood is a micropolar fluid.

2. **Industrial Processes:**In number of industrial processes, MP fluids are used and MMR can play a vital role in improving these processes.

In conclusion, the interplay between magnetization and the microstructure of micropolar fluids in magnetic fields results in the phenomenon known as micromagnetorotation. It's a crucial idea in fluid mechanics that has ramifications for numerous engineering and scientific fields.

2.10.2 Micropolar Fluid

A fluid is said to be micropolar if it has microrotation in addition to the typical translational motion. This implies that the constituent particles of the fluid, which are more than just points but also include interior structure, are capable of rotating.

In contrast to conventional Newtonian fluids, which treat the particles as points devoid of internal degrees of freedom, this is a significant distinction.

2.10.3 Microrotation

In fluid mechanics,microrotation refers to rotational motion or spinning motion of the tiny particles that make up a fluid.

Chapter 3

Heat Transfer Model In Micropolar Continuum

3.1 Mathematical Model

The model presented below is considered with the assumption that pressure gradient is constant, flow is steady, incompressible and magnetic induced through a rectangular channel, as shown in Figure 3.1. Furthermore, $\frac{\partial P}{\partial z}$ is assumed constant and a magnetic field of magnitude Bo is applied in the direction of flow. The pressure gradient is taking a constant value in order to derive the flow down through the channel in z-direction. In order to maintain a constant temperature at the walls of the considered channel, for velocity slip, convective thermal boundary conditions, and a channel width that spans along the $x-$ and $y-$ axis, the coordinate system is selected. Let $\boldsymbol{\omega} = \omega_x \hat{i} + \omega_y \hat{j}$ be the MR velocity vector and $\mathbf{u} = u_z(x, y)\hat{k}$ be the MP fluid velocity vector. Furthermore, suppose that a high magnetic Reynolds number (Rm) results in a sizable induced magnetic field. When body force and couplings are not present, the governing PDEs of the physical system dynamics are as follows:

When body force and couplings are not present, the governing system of dynamical equations is as follows:

$$\frac{\partial \rho}{\partial t} + \nabla \cdot (\rho \mathbf{u}) = 0, \tag{3.1}$$

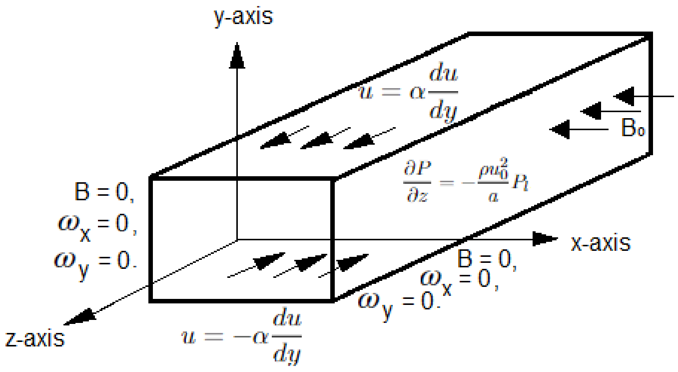

FIGURE 3.1: Schematic diagram of the computational domain.

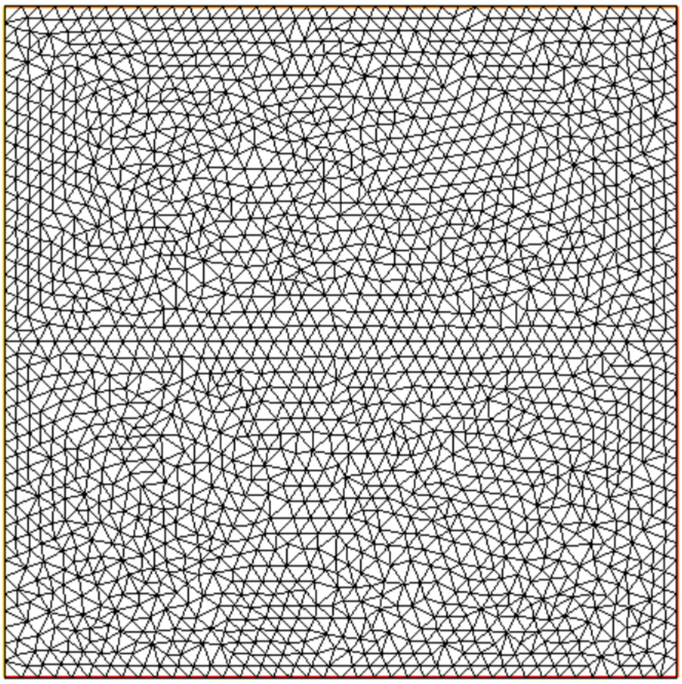

FIGURE 3.2: Schematic diagram of the computational domain.

$$\rho \frac{D\mathbf{u}}{Dt} = -\nabla P - (\mu + k)\nabla \times \nabla \times \mathbf{u} + k\nabla \times \boldsymbol{\omega} + \mathbf{J} \times \mathbf{B}, \tag{3.2}$$

$$\rho j^* \frac{D\boldsymbol{\omega}}{Dt} = k\nabla \times \mathbf{u} - 2k\boldsymbol{\omega} + (\tilde{\alpha} + \beta + \gamma)\nabla(\nabla \cdot \boldsymbol{\omega}) - \gamma\nabla \times (\nabla \times \boldsymbol{\omega}), \tag{3.3}$$

$$\rho C_{\mathrm{p}} \frac{DT}{Dt} = K_{\mathrm{f}}\nabla^2 T + \lambda (\nabla \cdot \mathbf{u})^2 + 2\mu(\mathbf{D} : \mathbf{D}) + 4k \left(\frac{1}{2}\nabla \times \mathbf{u} - \boldsymbol{\omega}\right)^2 + \tilde{\alpha} (\nabla \cdot \boldsymbol{\omega})$$
$$+ \gamma (\nabla\boldsymbol{\omega}) : (\nabla\boldsymbol{\omega})^T + \frac{\mathbf{J}}{\sigma} = 0. \tag{3.4}$$

where the fluid's pressure, temperature, and ρ are indicated by the parameters P, T, and ρ, respectively. Furthermore, the variables related to electrical conductivity, microgyration constant, specific heat at constant pressure, thermal conductivity, and electric current density are K_{f}, C_{p}, $\mathbf{J}$, j^* and σ, respectively. The strain rate tensor is represented by $\mathbf{D}$ in (3.4), which is defined as $\mathbf{D} = 0.5\left(\nabla \mathbf{u}^{\mathrm{T}} + \nabla \mathbf{u}\right)$. The entire magnetic field is represented by the vector $\mathbf{B} = (B_0\hat{i} + B_{\mathrm{z}}\hat{k})$. The following relations are satisfied by the material constants $\mu, k, \tilde{\alpha}, \beta$, and γ in (3.3).

$$k \geq 0, \quad 2\mu + k \geq 0, \quad 3\tilde{\alpha} + \gamma \geq 0, \quad \text{and} \quad \gamma \geq |\beta|. \tag{3.5}$$

Ohm's law is used to account for the relationship between the electric current density $\mathbf{J}$, magnetic field $\mathbf{B}$, and electric field density vector $\mathbf{E}$.

$$\mathbf{J} = \sigma(\mathbf{E} + \mathbf{u} \times \mathbf{B}), \tag{3.6}$$

the Maxwell's equations

$$\nabla \times \mathbf{B} = \mu_{\mathrm{m}}\mathbf{J}, \quad \nabla \times \mathbf{E} = \frac{\partial \mathbf{B}}{\partial t}, \quad \nabla \cdot \mathbf{E} = 0, \quad \nabla \cdot \mathbf{B} = 0, \tag{3.7}$$

and induction equation

$$\frac{\partial \mathbf{B}}{\partial t} = \nabla \times (\mathbf{u} \times \mathbf{B}) + \frac{1}{\sigma \mu_{\mathrm{m}}}\nabla^2 \mathbf{B}. \tag{3.8}$$

The electric field density $\mathbf{E}$ is believed to be insignificant in this instance. The component forms of the equations in (3.2) through (3.4) are as follows:

$$B_0\left(\frac{\partial u^{\mathrm{z}}}{\partial x}\right) + \frac{1}{\sigma \mu_m}\left(\frac{\partial^2 B^{\mathrm{z}}}{\partial x^2} + \frac{\partial^2 B^{\mathrm{z}}}{\partial y^2}\right) = 0, \tag{3.9}$$

$$-\frac{\partial P}{\partial Z} + (\mu + k)\left(\frac{\partial^2 u^{\mathrm{z}}}{\partial x^2} + \frac{\partial^2 u^{\mathrm{z}}}{\partial y^2}\right) + k\left(\frac{\partial \omega^{\mathrm{y}}}{\partial x} - \frac{\partial \omega^{\mathrm{x}}}{\partial y}\right) + \frac{B_0}{\mu_m}\left(\frac{\partial B^{\mathrm{z}}}{\partial x}\right) = 0, \tag{3.10}$$

$$-2k\omega^{\mathrm{x}} + k\frac{\partial u^{\mathrm{z}}}{\partial y} + \gamma\frac{\partial}{\partial y}\left(\frac{\partial \omega^{\mathrm{x}}}{\partial y} - \frac{\partial \omega^{\mathrm{y}}}{\partial x}\right) + (\tilde{\alpha} + \beta + \gamma)\frac{\partial}{\partial x}\left(\frac{\partial \omega^{\mathrm{x}}}{\partial x} + \frac{\partial \omega^{\mathrm{y}}}{\partial y}\right) = 0, \tag{3.11}$$

$$-2k\omega^{\mathrm{y}} + k\frac{\partial u^{\mathrm{z}}}{\partial x} + \gamma\frac{\partial}{\partial x}\left(\frac{\partial \omega^{\mathrm{y}}}{\partial x} - \frac{\partial \omega^{\mathrm{x}}}{\partial y}\right) + (\tilde{\alpha} + \beta + \gamma)\frac{\partial}{\partial y}\left(\frac{\partial \omega^{\mathrm{x}}}{\partial x} + \frac{\partial \omega^{\mathrm{y}}}{\partial y}\right) = 0, \tag{3.12}$$

$$
\begin{aligned}
k_f\Big(\frac{\partial^2 T}{\partial x^2}+\frac{\partial^2 T}{\partial y^2}\Big)&+(\mu+k)\Big\{\Big(\frac{\partial u^{\mathrm{z}}}{\partial x}\Big)^2+\Big(\frac{\partial u^{\mathrm{z}}}{\partial y}\Big)^2\Big\}+\tilde{\alpha}\Big(\frac{\partial \omega^{\mathrm{x}}}{\partial x}+\frac{\partial \omega^{\mathrm{y}}}{\partial y}\Big)^2\\
&+2k\Big((\omega^{\mathrm{x}})^2+(\omega^{\mathrm{y}})^2-\omega^{\mathrm{x}}\frac{\partial u^{\mathrm{z}}}{\partial y}+\omega^{\mathrm{y}}\frac{\partial u^{\mathrm{z}}}{\partial x}\Big)\\
&+\gamma\Big\{\Big(\frac{\partial \omega^{\mathrm{x}}}{\partial x}\Big)^2+\Big(\frac{\partial \omega^{\mathrm{x}}}{\partial y}\Big)^2+\Big(\frac{\partial \omega^{\mathrm{y}}}{\partial x}\Big)^2+\Big(\frac{\partial \omega^{\mathrm{y}}}{\partial y}\Big)^2\Big\}\\
&+\beta\Big\{\Big(\frac{\partial \omega^{\mathrm{x}}}{\partial x}\Big)^2+\Big(\frac{\partial \omega^{\mathrm{y}}}{\partial y}\Big)^2+\Big(\frac{\partial \omega^{\mathrm{x}}}{\partial y}\frac{\partial \omega^{\mathrm{y}}}{\partial x}\Big)\Big\}\\
&+\frac{1}{\sigma\mu_m^2}\Big(\frac{\partial^2 B^{\mathrm{z}}}{\partial x^2}+\frac{\partial^2 B^{\mathrm{z}}}{\partial y^2}\Big)=0.
\end{aligned}
\tag{3.13}
$$

The conditions at the boundaries, of the considered geometry, are described as:

$$
\begin{cases}
B=0, \quad u^{\mathrm{z}}=0, \quad \omega^{\mathrm{x}}=0, \quad \omega^{\mathrm{y}}=0, & \text{at} \quad \mathrm{x=z=0} \quad \textit{and} \quad \mathrm{(x, z)=(a, l)},\\
B=0, \quad \omega^{\mathrm{x}}=0, \quad \omega^{\mathrm{y}}=0, \quad \theta=0, & \text{at} \quad \mathrm{y=z=0} \quad \text{and} \quad \mathrm{(y, z)=(b, l)},\\
u^{\mathrm{z}}=\alpha^*\dfrac{du^{\mathrm{z}}}{dy} & \text{at} \quad \mathrm{y{=}0} \quad \textit{and} \quad \mathrm{y{=}b},\\
k_f\dfrac{dT}{dx}-h(T-T_f)=0, & \text{at} \quad x=0,\\
k_f\dfrac{dT}{dx}+h(T-T_w)=0, & \text{at} \quad x=a.
\end{cases}
\tag{3.14}
$$

Here α^* represents the slip coefficient.

To get the non-dimensional states, following variables are used:

$$
\begin{gathered}
X=\frac{x}{a}, \quad Y=\frac{y}{a}, \quad u=\frac{u^{\mathrm{z}}}{u_0}, \quad \omega_1=\frac{\omega^{\mathrm{x}}a}{u_0}, \quad \omega_2=\frac{\omega^{\mathrm{y}}a}{u_0}, \quad B=\frac{B_z}{B_0},\\
\theta=\frac{T-T_w}{T_f-T_w}, \quad \text{and} \quad \frac{\partial P}{\partial z}=-\frac{\rho u_0^2}{a}P_l.
\end{gathered}
\tag{3.15}
$$

Using the transformations from in equations (3.9) to (3.14), we arrive at

$$
\frac{\partial u}{\partial X}+\frac{1}{Rm}\Big(\frac{\partial^2 B}{\partial X^2}+\frac{\partial^2 B}{\partial Y^2}\Big)=0, \tag{3.16}
$$

$$R_eP_l + \Big(\frac{1}{1-N}\Big)\Big(\frac{\partial \omega_2}{\partial X} - \frac{\partial \omega_1}{\partial Y}\Big) + \Big(\frac{1}{1-N}\Big)\Big(\frac{\partial^2 u}{\partial X^2} + \frac{\partial^2 u}{\partial Y^2}\Big) + \frac{Ha^2}{Rm}\Big(\frac{\partial B}{\partial X}\Big) = 0, \quad (3.17)$$

$$\omega_1 - \frac{1}{2}\frac{\partial u}{\partial Y} - \left(\frac{2-N}{2m^2}\right)\frac{\partial^2 \omega_1}{\partial Y^2} - \frac{1}{l^2}\frac{\partial^2 \omega_1}{\partial X^2} - \left(\frac{2m^2 - l^2(2-N)}{2m^2 l^2}\right)\frac{\partial^2 \omega_2}{\partial x \partial y} = 0, \quad (3.18)$$

$$\omega_2 + \frac{1}{2}\frac{\partial u}{\partial x} - \left(\frac{2-N}{2m^2}\right)\frac{\partial^2 \omega_2}{\partial x^2} - \frac{1}{l^2}\frac{\partial^2 \omega_2}{\partial y^2} - \left(\frac{2m^2 - l^2(2-N)}{2m^2 l^2}\right)\frac{\partial^2 \omega_1}{\partial x \partial y} = 0, \quad (3.19)$$

$$\begin{aligned} &\left(\frac{\partial^2 \theta}{\partial X^2} + \frac{\partial^2 \theta}{\partial Y^2}\right) + Br\Bigg[\left(\frac{1}{1-N}\right)^2 \left(\left(\frac{\partial u}{\partial X}\right)^2 + \left(\frac{\partial u}{\partial Y}\right)^2\right) \\ &+ \left(\frac{2N}{1-N}\right)\left(\omega_1^2 + \omega_2^2 - \omega_1 \frac{\partial v}{\partial Y} + \omega_2 \frac{\partial v}{\partial X}\right) \\ &+ A\left(\frac{\partial \omega_1}{\partial X} + \frac{\partial \omega_2}{\partial Y}\right)^2 + \left(\frac{N(2-N)}{m^2(1-N)}\right) \\ &\cdot \left\{\left(\frac{\partial \omega_1}{\partial X}\right)^2 + \left(\frac{\partial \omega_1}{\partial Y}\right)^2 + \left(\frac{\partial \omega_2}{\partial X}\right)^2 + \left(\frac{\partial \omega_2}{\partial Y}\right)^2\right\} \\ &+ C\left\{\left(\frac{\partial \omega_1}{\partial X}\right)^2 + \left(\frac{\partial \omega_2}{\partial Y}\right)^2 + 2\frac{\partial \omega_1}{\partial Y}\frac{\partial \omega_1}{\partial X}\right\}\Bigg] \\ &+ \frac{Ha^2 Br}{R_m^2}\left(\frac{\partial^2 B}{\partial X^2} + \frac{\partial^2 B}{\partial Y^2}\right) = 0. \end{aligned} \quad (3.20)$$

where Rm, Br, Re, Ha and N denote the magnetic Reynolds, Brinkmann number, Reynolds, Hartmann number, Coupling numbers respectively.

Above numbers are given as:

$$\begin{aligned} &R_e = \rho\frac{u_0 a}{\mu}, \quad R_m = \sigma \mu_m u_0 a, \quad Ha = B_0 a\sqrt{\frac{\sigma}{\mu}}, \quad N = \frac{k}{\mu + k}, \\ &Br = \frac{\mu u_0^2}{k_f(T_f - T_w)}. \end{aligned} \quad (3.21)$$

whereas, $m^2 = \frac{a^2k(2\mu+k)}{\gamma(\mu+k)}$, $A = \frac{\tilde{\alpha}}{\mu a^2}$, $C = \frac{\beta}{\mu a^2}$ and $l^2 = \frac{2a^2k}{\tilde{\alpha}+\beta+\gamma}$ show the non-dimensional and micropolar properties associated with the microstructure of the material.

The inverted gradient pressure in equation (17) is $P_l = (\frac{\partial P}{\partial Z})^{-1}$. The boundary conditions are recasted as follows, following the transformation in (3.15):

$$\begin{cases} B = 0, \quad u = 0, \quad \omega_1 = 0, \quad \omega_2 = 0, \quad \text{at} \quad x = z = 0 \quad \text{and} \quad x = z = 1, \\ B = 0, \quad \omega_1 = 0, \quad \omega_2 = 0, \quad \theta = 0, \quad \text{at} \quad y = z = 0 \quad \text{and} \quad y = y_0, \\ \dfrac{d\theta}{dx} - Bi(\theta - 1) = 0 \quad \text{at} \quad x = 0, \\ \dfrac{d\theta}{dx} - Bi\theta = 0 \quad \text{at} \quad x = 1, \\ u = -\alpha\dfrac{du}{dy}, \qquad \text{at} \quad y = 0, \\ u = \alpha\dfrac{du}{dy}, \qquad \text{at} \quad y = y_0. \end{cases} \tag{3.22}$$

where

$y_0 = \frac{b}{a}$ is aspect ratio,

$\alpha = \frac{\tilde{\alpha}}{a}$ is slip flow,

and

$B_i = \frac{ah}{k_f}$ is slip convection parameters.

3.2 Variational Formulation

Below is a representation of the variational model of induced magnetic micropolar flow. To

address the problem in Equations (3.16–3.22) on triangulation Ω^{h}, the domain Ω will now be descretized using triangular elements K_i. This will ensure that

$$\Omega^h := \bigcup_{i=1}^{ne} K_i$$

where "ne" is the number of quantity of finite element $K_i \in \Omega^h$ is the i^{th} triangular element in

descretized net satisfying the following property:

$$K_i \cap K_j = \emptyset, \quad \text{for} \quad i \neq j. \tag{3.23}$$

Now finite element spaces are defined:

$$U^h \times \Theta^h = \{(u,\theta) \in H_1(\Omega)|\, \forall\, K \in \Omega^h \quad u|^k \in P_2 \quad \theta|^K \in P_2\}, \tag{3.24}$$

and

$$B^h \times W^h = \{(B, w^i) \in H_1(\Omega) \times H_1(\Omega)|\, \forall\, K \in \Omega^h \quad B|^K \in P_2 \quad w^i|^K \in P_2; i = 1, 2\}. \tag{3.25}$$

In (3.24), P_2 is polynomials' set in $\mathbb{R}^2$, with degree ≤ 2 and $H_1(\Omega)$ being Sobolev space defined by

$$H_1(\Omega) := \{g \in L_2(\Omega); \quad \partial_k g \in L_2(\Omega)\ (k \in \{1, ..., n\})\}.$$

In this case, n stands for the dimension, and L_2 has its typical norm.

Sobolev space is embedded with the following norm:

$$||g||_2 := \left(||g||_2^2 + \sum_{j=1}^{n} ||\partial_j g||_2^2 \right)^{1/2}.$$

3.3 Finite Element Setting of Weak Problem

The weak form in integral representation of the considered problem in equations (3.16-3.22), are:

Find $\{u, \theta, B, w^1, w^2\} \in \{\mathbf{U}^h \times \Theta^h \times B^h \times W^h\}$, such that

$$\frac{\partial u}{\partial X} + \frac{1}{Rm}\Big(\frac{\partial^2 B}{\partial X^2} + \frac{\partial^2 B}{\partial Y^2}\Big) = 0. \tag{3.26}$$

Multiply above equation with weight function $\tilde{B}$ and integrate over the domain Ω.

$$\int_\Omega \tilde{B} \cdot \left[\frac{\partial u}{\partial X} + \frac{1}{Rm}\Big(\frac{\partial^2 B}{\partial X^2} + \frac{\partial^2 B}{\partial Y^2}\Big)\right] d\Omega = 0, \tag{3.27}$$

$$\Rightarrow \int_\Omega \frac{\partial u^{n+1}}{\partial X^{n+1}} \cdot \tilde{B} d\Omega + \frac{1}{R_m}\int_\Omega \nabla B_{n+1} \cdot \nabla \tilde{B} = 0, \quad \forall \ \tilde{B} \in B^h, \tag{3.28a}$$

$$R_e P_l + \Big(\frac{1}{1-N}\Big)\Big(\frac{\partial \omega_2}{\partial X} - \frac{\partial \omega_1}{\partial Y}\Big) + \Big(\frac{1}{1-N}\Big)\Big(\frac{\partial^2 u}{\partial X^2} + \frac{\partial^2 u}{\partial Y^2}\Big) + \frac{Ha^2}{Rm}\Big(\frac{\partial B}{\partial X}\Big) = 0. \tag{3.28b}$$

Multiply above equation with weight function $\tilde{u}$ and integrate over the domain Ω.

$$\int_\Omega \tilde{u} \cdot \left[R_e P_l + \Big(\frac{1}{1-N}\Big)\Big(\frac{\partial \omega_2}{\partial X} - \frac{\partial \omega_1}{\partial Y}\Big) + \Big(\frac{1}{1-N}\Big)\Big(\frac{\partial^2 u}{\partial X^2} + \frac{\partial^2 u}{\partial Y^2}\Big) + \frac{Ha^2}{Rm}\Big(\frac{\partial B}{\partial X}\Big)\right] = 0, \tag{3.28c}$$

$$\begin{aligned} \int_\Omega (R_e P_l) \cdot \tilde{u} d\Omega + \left(1 + \frac{1}{1+(-N)}\right) \int_\Omega \left(\frac{\partial \omega_2^{n+1}}{\partial X^{n+1}} + \frac{\partial \omega_1^{n+1}}{\partial Y^{n+1}}\right) \cdot \tilde{u} \\ - \left(\frac{1}{1+(-N)}\right) \int_\Omega (\nabla u^{n+1} \cdot \nabla \tilde{u}) d\Omega \\ + \frac{Ha^2}{R_m} \int_\Omega \frac{\partial B^{n+1}}{\partial X^{n+1}} \cdot \tilde{u} = 0, \quad \forall \ \tilde{u} \in U^h, \end{aligned} \tag{3.28d}$$

$$\omega_1 - \frac{1}{2}\frac{\partial u}{\partial Y} - \left(\frac{2-N}{2m^2}\right)\frac{\partial^2 \omega_1}{\partial Y^2} - \frac{1}{l^2}\frac{\partial^2 \omega_1}{\partial X^2} - \left(\frac{2m^2 - l^2(2-N)}{2m^2 l^2}\right)\frac{\partial^2 \omega_2}{\partial x \partial y} = 0. \tag{3.28e}$$

Multiply above equation with weight function $\tilde{\omega}_1$ and integrate over the domain Ω.

$$\int_\Omega \tilde{\omega}_1 \cdot \left[\omega_1 - \frac{1}{2}\frac{\partial u}{\partial Y} - \left(\frac{2-N}{2m^2}\right)\frac{\partial^2 \omega_1}{\partial Y^2} - \frac{1}{l^2}\frac{\partial^2 \omega_1}{\partial X^2} - \left(\frac{2m^2 - l^2(2-N)}{2m^2 l^2}\right)\frac{\partial^2 \omega_2}{\partial x \partial y}\right] d\Omega = 0, \tag{3.28f}$$

$$\begin{aligned}-\frac{1}{2}\int_{\Omega}\frac{\partial u^{n+1}}{\partial Y^{n+1}}\cdot\tilde{\omega}_1 d\Omega+\Big(\frac{2m^2+(-l^2(2-N))}{2m^2l^2}\Big)\int_{\Omega}\frac{\partial\omega_2^{n+1}}{\partial Y^{n+1}}\cdot\frac{\partial\tilde{\omega}_1}{\partial X^{n+1}}d\Omega\\+\Big(\frac{1}{l^2}\Big)\int_{\Omega}\frac{\partial\omega_2^{n+1}}{\partial X^{n+1}}\cdot\frac{\partial\tilde{\omega}_1}{\partial X^{n+1}}d\Omega\\+\Big(\frac{2+(-N))}{2m^2}\Big)\int_{\Omega}\frac{\partial\omega_1^{n+1}}{\partial Y^{n+1}}\cdot\frac{\partial\tilde{\omega}_1}{\partial Y^{n+1}}d\Omega\\+\int_{\Omega}\omega_1^{n+1}\cdot\tilde{\omega}_1 d\Omega=0,\quad\forall\ \tilde{\omega_1}\in W_h,\end{aligned}\tag{3.28g}$$

$$\omega_2+\frac{1}{2}\frac{\partial u}{\partial x}-\left(\frac{2-N}{2m^2}\right)\frac{\partial^2\omega_2}{\partial x^2}-\frac{1}{l^2}\frac{\partial^2\omega_2}{\partial y^2}-\left(\frac{2m^2-l^2(2-N)}{2m^2l^2}\right)\frac{\partial^2\omega_1}{\partial x\partial y}=0.\tag{3.28h}$$

Multiply above equation with weight function $\tilde{\omega}_2$ and integrate over the domain Ω.

$$\int_{\Omega}\tilde{\omega}_2\cdot\left[\omega_2+\frac{1}{2}\frac{\partial u}{\partial x}-\left(\frac{2-N}{2m^2}\right)\frac{\partial^2\omega_2}{\partial x^2}-\frac{1}{l^2}\frac{\partial^2\omega_2}{\partial y^2}-\left(\frac{2m^2-l^2(2-N)}{2m^2l^2}\right)\frac{\partial^2\omega_1}{\partial x\partial y}\right]d\Omega=0,\tag{3.28i}$$

$$\begin{aligned}-\frac{1}{2}\int_{\Omega}\frac{\partial u^{n+1}}{\partial X^{n+1}}\cdot\tilde{\omega}_2 d\Omega+\Big(\frac{2m^2+(-l^2(2-N))}{2m^2l^2}\Big)\int_{\Omega}\frac{\partial\omega_1^{n+1}}{\partial Y^{n+1}}\cdot\frac{\partial\tilde{\omega}_2}{\partial X^{n+1}}d\Omega\\+\Big(\frac{1}{l^2}\Big)\int_{\Omega}\frac{\partial\omega_1^{n+1}}{\partial Y^{n+1}}\cdot\frac{\partial\tilde{\omega}_2}{\partial Y^{n+1}}d\Omega\\+\Big(\frac{2+(-N))}{2m^2}\Big)\int_{\Omega}\frac{\partial\omega_2^{n+1}}{\partial X^{n+1}}\cdot\frac{\partial\tilde{\omega}_2}{\partial X^{n+1}}d\Omega\\+\int_{\Omega}\omega_2^{n+1}\cdot\tilde{\omega}_2 d\Omega=0,\quad\forall\ \tilde{\omega_2}\in W_h,\end{aligned}\tag{3.28j}$$

$$\begin{aligned}\left(\frac{\partial^2\theta}{\partial X^2}+\frac{\partial^2\theta}{\partial Y^2}\right)+Br\Bigg[\left(\frac{1}{1-N}\right)^2\left(\left(\frac{\partial u}{\partial X}\right)^2+\left(\frac{\partial u}{\partial Y}\right)^2\right)\\+\left(\frac{2N}{1-N}\right)\left(\omega_1^2+\omega_2^2-\omega_1\frac{\partial v}{\partial Y}+\omega_2\frac{\partial v}{\partial X}\right)+A\left(\frac{\partial\omega_1}{\partial X}+\frac{\partial\omega_2}{\partial Y}\right)^2\\+\left(\frac{N(2-N)}{m^2(1-N)}\right)\left\{\left(\frac{\partial\omega_1}{\partial X}\right)^2+\left(\frac{\partial\omega_1}{\partial Y}\right)^2+\left(\frac{\partial\omega_2}{\partial X}\right)^2+\left(\frac{\partial\omega_2}{\partial Y}\right)^2\right\}\\+C\left(\left(\frac{\partial\omega_1}{\partial X}\right)^2+\left(\frac{\partial\omega_2}{\partial Y}\right)^2+2\frac{\partial\omega_1}{\partial Y}\frac{\partial\omega_1}{\partial X}\right)\Bigg]\\+\frac{Ha^2Br}{R_m^2}\left(\frac{\partial^2B}{\partial X^2}+\frac{\partial^2B}{\partial Y^2}\right)=0.\end{aligned}\tag{3.28k}$$

Multiply above equation with weight function $\tilde{\theta}$ and integrate over the domain Ω.

$$\int_{\Omega} \tilde{\theta} \cdot \Bigg[\left(\frac{\partial^2\theta}{\partial X^2} + \frac{\partial^2\theta}{\partial Y^2}\right) + Br\Bigg[\left(\frac{1}{1-N}\right)^2 \left(\left(\frac{\partial u}{\partial X}\right)^2 + \left(\frac{\partial u}{\partial Y}\right)^2\right)$$
$$+ \left(\frac{2N}{1-N}\right)\left(\omega_1^2 + \omega_2^2 - \omega_1\frac{\partial v}{\partial Y} + \omega_2\frac{\partial v}{\partial X}\right)$$
$$+ A\left(\frac{\partial\omega_1}{\partial X} + \frac{\partial\omega_2}{\partial Y}\right)^2 + \left(\frac{N(2-N)}{m^2(1-N)}\right)\left(\left(\frac{\partial\omega_1}{\partial X}\right)^2 + \left(\frac{\partial\omega_1}{\partial Y}\right)^2 + \left(\frac{\partial\omega_2}{\partial X}\right)^2 + \left(\frac{\partial\omega_2}{\partial Y}\right)^2\right)$$
$$+ C\Bigg(\left(\frac{\partial\omega_1}{\partial X}\right)^2$$
$$+ \left(\frac{\partial\omega_2}{\partial Y}\right)^2 + 2\frac{\partial\omega_1}{\partial Y}\frac{\partial\omega_1}{\partial X}\Bigg)\Bigg]$$
$$+ \frac{Ha^2Br}{R_m^2}\left(\frac{\partial^2 B}{\partial X^2} + \frac{\partial^2 B}{\partial Y^2}\right)\Bigg]d\Omega = 0. \tag{3.28l}$$

we get,

$$Br\Bigg[\frac{1}{1+(-N)}\Bigg(\frac{\partial u^n}{\partial X^n}\cdot\frac{\partial u^{n+1}}{\partial X^{n+1}}$$
$$+ \frac{\partial u^n}{\partial Y^n}\cdot\frac{\partial u^{n+1}}{\partial Y^{n+1}}\Bigg)\cdot\tilde{\theta} \tag{3.28m}$$
$$+ \left(\frac{2N}{1+(-N)}\right)\left\{\omega_1^n\left(\omega_1^{n+1} - \frac{\partial V^{n+1}}{\partial Y^{n+1}} + \omega_2^n\left(\omega_2^{n+1} + \frac{\partial V^{n+1}}{\partial X^{n+1}}\right)\right)\right\}\cdot\tilde{\theta}$$
$$+ A\left(\frac{\partial\omega_1^n}{\partial X^n} + \frac{\partial\omega_2^n}{\partial Y^n}\right)\left(\frac{\partial\omega_1^{n+1}}{\partial X^{n+1}} + \frac{\partial\omega_2^{n+1}}{\partial Y^{n+1}}\right)\cdot\tilde{\theta} \tag{3.28n}$$
$$+\left(\frac{N(2-N)}{m^2(1-N})\right)\left(\frac{\partial\omega_1^n}{\partial X^n}\frac{\partial\omega_1^{n+1}}{\partial X^{n+1}} + \frac{\partial\omega_1^n}{\partial Y^n}\frac{\partial\omega_1^{n+1}}{\partial Y^{n+1}} + \frac{\partial\omega_2^n}{\partial X^n}\frac{\partial\omega_2^{n+1}}{\partial X^{n+1}} + \frac{\partial\omega_2^n}{\partial Y^n}\frac{\partial\omega_2^{n+1}}{\partial Y^{n+1}}\right)\cdot\tilde{\theta}\Bigg]$$
$$+ \frac{\partial\theta^{n+1}}{\partial X^{n+1}}\frac{\partial\tilde{\theta}}{\partial X^{n+1}}$$
$$+ \frac{\partial\theta^{n+1}}{\partial Y^{n+1}}\frac{\partial\tilde{\theta}}{\partial Y^{n+1}} \tag{3.28o}$$
$$+ \frac{Ha^2Br}{R_m^2}\left(\frac{\partial B^{n+1}}{\partial X^{n+1}}\frac{\partial\tilde{\theta}}{\partial X^{n+1}} + \frac{\partial B^{n+1}}{\partial Y^{n+1}}\frac{\partial\tilde{\theta}}{\partial Y^{n+1}}\right) = 0, \quad \forall\ \tilde{\theta}\in\Theta^h.$$

subjected to the boundary conditions

$$\begin{cases} B^{n+1} = 0, \quad u^{n+1} = 0, \quad \omega_1^{n+1} = 0, \quad \omega_2^{n+1} = 0, \\ \quad \text{at} \quad X^{n+1} = 0 \quad \text{and} \quad X^{n+1} = 1, \\ B^{n+1}=0, \quad u^{n+1}=0, \quad \omega_1^{n+1}=0, \quad \omega_2^{n+1}=0, \quad \theta^{n+1}=0, \quad \text{at} \quad Z^{n+1}=0 \quad \text{and} \quad Z^{n+1}=1, \\ \dfrac{d\theta^{n+1}}{dX^{n+1}} - Bi(\theta^{n+1} - 1) = 0 \quad \text{at} \quad X^{n+1} = 0, \\ \dfrac{d\theta^{n+1}}{dX^{n+1}} - Bi\theta^{n+1} = 0 \quad \text{at} \quad X^{n+1} = 1, \\ B^{n+1} = 0, \quad \theta^{n+1} = 0, \quad \omega_1^{n+1} = 0, \quad \omega_2^{n+1} = 0, \\ \quad \text{at} \quad Y^{n+1} = 0 \quad \text{and} \quad Y^{n+1} = Y_0^{n+1}, \\ u^{n+1} = -\alpha \dfrac{du^{n+1}}{dY^{n+1}} \quad \text{at} \quad Y^{n+1} = 0, \\ u^{n+1} = \alpha \dfrac{du^{n+1}}{dY^{n+1}} \quad \text{at} \quad Y^{n+1} = Y_0^{n+1}. \end{cases}$$

Chapter 4

Effect of Micromagnetorotation

4.1 Mathematical Model in Micropolar Framework

Figure 4.1 illustrates a continuous, incompressible micropolar magnetic fluid flow in a square cavity. To study the effect of MMR on the thermal,velocity and microrotational velocity of present flow system, a model presented by Khan and Isma [16] is studied. This is the extension of their work by including effect of MMR. The flow is just because of a constant pressure gradient $\frac{\partial P}{\partial Z}$, and $\mathbf{M} \times \mathbf{H}$ is magnetization effect on microrotation. It is anticipated that a steady pressure gradient will cause the flow to begin along the cavity in the xy direction. The cavity's length runs along the x and y axes as adopted by coordinate system. The width of cavity is stretched along x-axis and y-axis. The temperature is maintained at a constant level along the channel wall. At the walls, connected thermal boundary conditions and velocity drop are employed. Let $\mathbf{u} = (0, 0, u_z)$ be the vector of velocity for micropolar fluids and $\omega = \omega_x \hat{i} + \omega_y \hat{j}$, represents the microrotational velocity vector in x-direction and y-direction. Further, assume that when body force and couplings are not present, the governing PDEs system of equations describing the dynamics of the flow is as follows:

$$\frac{\partial \rho}{\partial t} + \nabla \cdot (\rho \mathbf{u}) = 0, \tag{4.1}$$

$$\rho \frac{D\mathbf{u}}{Dt} = -\nabla P - (\mu + k)\nabla \times \nabla \times \mathbf{u} + k\nabla \times \omega + \mathbf{J} \times \mathbf{B}, \tag{4.2}$$

$$\rho j^* \frac{D\omega}{Dt} = k\nabla \times \mathbf{u} - 2k\omega + (\alpha + \beta + \gamma)\nabla(\nabla \cdot \omega) - \gamma\nabla \times (\nabla \times \omega) + \mathbf{M} \times \mathbf{H}, \quad (4.3)$$

$$\begin{aligned} \rho \mathbf{C}_P \frac{DT}{Dt} =& K_f \nabla^2 T + \lambda(\nabla \cdot \mathbf{U}^2) + 2\lambda(\mathbf{D} : \mathbf{D}) + 4k(\frac{1}{2}\nabla \times \mathbf{U} - \omega)^2 + \alpha(\nabla \cdot \omega) \\ & + \gamma(\nabla\omega) : (\nabla\omega)^T + (\tau \frac{M_0}{\mathbf{H}})(\omega \times \mathbf{H})^2 = 0. \end{aligned} \quad (4.4)$$

where the parameters ρ, T and P denote the density, temperature and pressure of the fluids, respectively. Furthermore, J, J^*, C_p, K_f and the characteristics associated with specific heat at constant pressure, electric current density, microgyration constant, electrical conductivity, and thermal conductivity are denoted by σ. Strain rate tensor D is defined as $\mathbf{D} = 0.5(\nabla \mathbf{u} + \nabla \mathbf{u}^T$ in equation (4.4). The vector $\mathbf{H} = (H_0 \hat{\imath} + H_y \hat{\jmath})$ is the magnetization factor . In (4.3), the material parameters μ, k, τ, ξ, M_P, $\tilde{\alpha}$, β and γ satisfy the following relations

$$k \geq 0, 2\mu + k \geq 0, 3\alpha + \gamma \geq 0, and \gamma \geq \left|\beta\right|. \quad (4.5)$$

Ohm's law is used to account for the link between the electric current density J, magnetic field B, and electric field density vector E.

$$\mathbf{J} = \sigma(\mathbf{E} + \mathbf{u} \times \mathbf{B}), \quad (4.6)$$

the Maxwell's equations

$$\nabla \times \mathbf{B} = \mu_m \mathbf{J}, \nabla \times \mathbf{E} = \frac{\partial \mathbf{B}}{\partial t}, \nabla \cdot \mathbf{E} = 0, \nabla \cdot \mathbf{B} = 0, \quad (4.7)$$

and the induction equation

$$\frac{\partial \mathbf{B}}{\partial t} = \nabla \times (\mathbf{u} \times \mathbf{B}) + \frac{1}{\sigma \mu_{\mathrm{m}}} \nabla^2 \mathbf{B}. \quad (4.8)$$

The electric field density **E** is believed to be insignificant in this instance. The component forms of the equations in (4.1) to (4.4) are as follows:

$$\begin{aligned}\mu_0 H_0 + M_0\left(\frac{\partial u_z}{\partial x}\right) + \frac{1}{\sigma\mu_m}\mu_0\left(\frac{\partial^2 H_z}{\partial x^2}\right) + \mu_0\left(\frac{\partial^2 H_z}{\partial y^2}\right)\\ + \frac{M_0}{\bar{H}}\left\{\frac{\partial^2 H_z}{\partial x^2} - \tau\left(H_0\frac{\partial^2 \omega_{\mathrm{y}}}{\partial x^2} - H_z\frac{\partial^2 \omega_x}{\partial x^2} - \omega_x\frac{\partial^2 H_z}{\partial x^2}\right)\right\}\\ + \frac{M_0}{\bar{H}}\left\{\frac{\partial^2 H_z}{\partial y^2} - \tau\left(H_0\frac{\partial^2 \omega_y}{\partial y^2} - H_z\frac{\partial^2 \omega_x}{\partial y^2} - \omega_x\frac{\partial^2 H_z}{\partial y^2}\right)\right\} = 0,\end{aligned} \tag{4.9}$$

$$\begin{aligned}-\frac{\partial P}{\partial z} + (\mu+k)\left(\frac{\partial^2 u_z}{\partial x^2} + \frac{\partial^2 u_z}{\partial y^2}\right) + k\left(\frac{\partial \omega_y}{\partial x} - \frac{\partial \omega_x}{\partial y}\right) + \frac{B_0}{\mu_m}\left(\frac{\partial B_z}{\partial x}\right)\\ - \left(\frac{M_0\tau H_0}{\bar{H}}\right)H_z\omega_y = 0.\end{aligned} \tag{4.10}$$

$$-2k\omega_x + k\frac{\partial u_{\mathrm{z}}}{\partial y} + \gamma\frac{\partial}{\partial y}\left(\frac{\partial \omega_x}{\partial y} - \frac{\partial \omega_y}{\partial x}\right) + (\tilde{\alpha}+\beta+\gamma)\frac{\partial}{\partial x}\left(\frac{\partial \omega_x}{\partial x} + \frac{\partial \omega_y}{\partial y}\right) = 0, \tag{4.11}$$

$$-2k\omega_y + k\frac{\partial u_z}{\partial x} - \gamma\frac{\partial}{\partial x}\left(\frac{\partial \omega_y}{\partial x} - \frac{\partial \omega_x}{\partial y}\right) + (\tilde{\alpha}+\beta+\gamma)\frac{\partial}{\partial y}\left(\frac{\partial \omega_x}{\partial x} + \frac{\partial \omega_y}{\partial y}\right) = 0, \tag{4.12}$$

and

$$\begin{aligned}k_f\left(\frac{\partial^2 T}{\partial x^2} + \frac{\partial^2 T}{\partial y^2}\right) + (\mu+k)\left\{\left(\frac{\partial u_z}{\partial x}\right)^2 + \left(\frac{\partial u_z}{\partial y}\right)^2\right\}\\ + \tilde{\alpha}\left(\frac{\partial \omega_x}{\partial x} + \frac{\partial \omega_y}{\partial y}\right)^2\\ + 2k\left(\omega_x^2 + \omega_y^2 - \omega_x\frac{\partial u_z}{\partial y} + \omega_y\frac{\partial u_z}{\partial x}\right)\\ + \gamma\left\{\left(\frac{\partial \omega_x}{\partial x}\right)^2 + \left(\frac{\partial \omega_x}{\partial y}\right)^2 + \left(\frac{\partial \omega_y}{\partial x}\right)^2 + \left(\frac{\partial \omega_y}{\partial y}\right)^2\right\}\\ + \beta\left\{\left(\frac{\partial \omega_x}{\partial x}\right)^2 + \left(\frac{\partial \omega_y}{\partial y}\right)^2 + \left(\frac{\partial \omega_x}{\partial y}\frac{\partial \omega_y}{\partial x}\right)\right\}\\ + (\omega_y H_z)^2 + (\omega_x H_z)^2 + (H_0\omega_y)^2 = 0,\end{aligned} \tag{4.13}$$

$$\frac{dH_z}{dt} + \mathbf{u}\frac{\partial H_z}{\partial Z} = \gamma\left(\frac{\partial^2 H_z}{\partial x^2} + \frac{\partial^2 H_z}{\partial y^2}\right) + \left(H_x\frac{\partial U_z}{\partial x} + H_z\frac{\partial U_z}{\partial Z}\right). \tag{4.14}$$

The linked flow problem's boundary conditions are explained as follows:

$$\begin{cases} \textbf{At Top}: u = -\alpha\frac{du}{dy}, \quad H = \omega_x = \omega_y = 0, \quad \forall \ (x,y) \in T \\ \text{where} \quad T := \{(x, 0.5) : -0.5 \leq x \leq 0.5\} \\ \textbf{At Right and Left of the Cavity}: u_z = H = \omega_x = \omega_y = 0, \\ \quad \forall \ (x,y) \in \mathbb{R}t \quad \text{and} \quad \forall \ (x,y) \in L \\ \quad \text{where} \quad \mathbb{R}t := \{(0.5, y) : -0.5 \leq y \leq 0.5\} \quad \text{and} \\ \quad L := \{(-0.5, y) : -0.5 \leq y \leq 0.5\} \\ \textbf{At Bottom of the Cavity}: u_z = \alpha\frac{du}{dy}, \quad H = \omega_x = \omega_y = 0, \quad \forall \ (x,y) \in Bt \\ \text{where} \quad Bt := \{(x, -0.5) : -0.5 \leq x \leq 0.5\} \end{cases} \tag{4.15}$$

Here, α denote the constant. To obtain the non-dimensional form, following variables are used:

$$X = \frac{x}{a}, \quad Y = \frac{y}{a}, \quad u = \frac{u_z}{u_0}, \quad \omega_1 = \frac{\omega_x a}{u_0}, \quad \omega_2 = \frac{\omega_y a}{u_0}, \quad H = \frac{H_z}{H_0}, \quad \theta = \frac{T - T_w}{T_f - T_w}, \\ \frac{\partial P}{\partial z} = -\frac{\rho u_0^2}{a} P_l. \tag{4.16}$$

Using the transformations from (4.16) in equations (4.9) to (4.14), we arrive at

$$\frac{\partial u}{\partial X} + \frac{h}{R_m}\left(\frac{\partial^2 H}{\partial X^2} + \frac{\partial^2 H}{\partial Y^2}\right) + \frac{h_\tau}{R_m}\left[H\left(\frac{\partial^2 \omega_1}{\partial x^2} + \frac{\partial^2 \omega_1}{\partial y^2}\right) + 2\left(\frac{\partial H}{\partial X}\frac{\partial \omega_1}{\partial X} + \frac{\partial \omega_1}{\partial Y}\frac{\partial \omega_1}{\partial Y}\right) \right. \\ \left. + \omega_1\left(\frac{\partial^2 H}{\partial X^2} + \frac{\partial^2 H}{\partial Y^2}\right) - \left(\frac{\partial^2 \omega_2}{\partial X^2} + \frac{\partial^2 \omega_2}{\partial Y^2}\right)\right] = 0, \tag{4.17}$$

$$R_eP_l+\left(\frac{1}{1-N}\right)\left(\frac{\partial^2 u}{\partial X^2}+\frac{\partial^2 u}{\partial Y^2}\right)+\left(\frac{1}{1-N}\right)\left(\frac{\partial \omega_2}{\partial X}-\frac{\partial \omega_1}{\partial Y}\right)+\xi h(\frac{\partial H}{\partial X})$$
$$+\xi h_\tau\left(H\frac{\partial \omega_1}{\partial X}+\omega_1\frac{\partial H}{\partial X}-\frac{\partial \omega_2}{\partial X}\right)=0, \tag{4.18}$$

$$\omega_1-\frac{1}{2}\frac{\partial u}{\partial Y}-\left(\frac{2-N}{2m^2}\right)\frac{\partial^2 \omega_1}{\partial Y^2}-\frac{1}{l^2}\frac{\partial^2 \omega_1}{\partial X^2}-\left(\frac{2m^2-l^2(2-N)}{2m^2l^2}\right)\frac{\partial^2 \omega_2}{\partial x\partial y}$$
$$-\frac{\alpha_1}{2}h_\tau\left(\frac{2-N}{m^2}\right)\omega_2H=0, \tag{4.19}$$

$$\omega_2+\frac{1}{2}\frac{\partial u}{\partial x}-\left(\frac{2-N}{2m^2}\right)\frac{\partial^2 \omega_2}{\partial x^2}-\frac{1}{l^2}\frac{\partial^2 \omega_2}{\partial y^2}-\left(\frac{2m^2-l^2(2-N)}{2m^2l^2}\right)\frac{\partial^2 \omega_1}{\partial x\partial y}$$
$$-\frac{\alpha_1}{2}h_\tau\left(\frac{2-N}{m^2}\right)\omega_2H=0, \tag{4.20}$$

$$\left(\frac{\partial^2 \theta}{\partial X^2}+\frac{\partial^2 \theta}{\partial Y^2}\right)+Br\left[\left(\frac{1}{1-N}\right)^2\left(\left(\frac{\partial u}{\partial X}\right)^2+\left(\frac{\partial u}{\partial Y}\right)^2\right)\right.$$
$$+\left(\frac{2N}{1-N}\right)\left(\omega_1^2+\omega_2^2-\omega_1\frac{\partial v}{\partial Y}+\omega_2\frac{\partial v}{\partial X}\right)$$
$$+A\left(\frac{\partial \omega_1}{\partial X}+\frac{\partial \omega_2}{\partial Y}\right)^2+\left(\frac{N(2-N)}{m^2(1-N)}\right)\left\{\left(\frac{\partial \omega_1}{\partial X}\right)^2+\left(\frac{\partial \omega_1}{\partial Y}\right)^2\right.$$
$$+\left(\frac{\partial \omega_2}{\partial X}\right)^2+\left(\frac{\partial \omega_2}{\partial Y}\right)^2$$
$$\left.\left.+C\left\{\left(\frac{\partial \omega_1}{\partial X}\right)^2+\left(\frac{\partial \omega_2}{\partial Y}\right)^2+2\left(\frac{\partial \omega_1}{\partial Y}\frac{\partial \omega_1}{\partial X}\right)\right\}\right]$$
$$+\frac{hM_p}{R_m^2}\left(\mu_0+\frac{M_0}{H}\right)\left(\frac{\partial^2 H}{\partial X^2}+\frac{\partial^2 H}{\partial Y^2}\right)+\frac{h_\tau M_p}{R_m^2}\left[H\left(\frac{\partial^2 \omega_1}{\partial X^2}+\frac{\partial^2 \omega_1}{\partial Y^2}\right)\right.$$
$$+2\left(\frac{\partial H}{\partial X}\frac{\partial \omega_1}{\partial X}+\frac{\partial H}{\partial Y}\frac{\partial \omega_2}{\partial Y}\right)+\omega_1\left(\frac{\partial^2 H}{\partial X^2}+\frac{\partial^2 H}{\partial Y^2}\right)$$
$$\left.-\left(\frac{\partial^2 \omega_1}{\partial X^2}+\frac{\partial^2 \omega_2}{\partial Y^2}\right)\right]=0. \tag{4.21}$$

where R_e, R_m, Ha, Al, Br, N, τ, ξ, h, h_τ and M_p denote the Renolds, magnetic

Reynolds, Hartmann, Brinkman, Relaxed magnetization factor, Relaxation time of magnetization, Magnetic ratio parameter, Magnetic parameter and coupling constant, respectively.

These constants are described as:

$$R_e = \rho\frac{u_0 a}{\mu}, \quad R_m = \sigma\mu_m\mu_0, \quad Ha = B_0 a\sqrt{\frac{\sigma}{\mu}}, \quad N = \frac{k}{\mu+k},$$
$$M_p = H_0 B_0 \mu_0^2, \quad \xi = \frac{B_0^2}{\mu\mu_m\mu_0}, \quad Br = \frac{\mu u_0^2}{k_f(T_f - T_w)}.$$

whereas, $m^2 = \dfrac{a^2 k(2\mu+k)}{\gamma(\mu+k)}$, $A = \dfrac{\tilde{\alpha}}{\mu a^2}$, $C = \dfrac{\beta}{\mu a^2}$ and $l^2 = \dfrac{2a^2 k}{\tilde{\alpha}+\beta+\gamma}$ represent micropolar and non-dimensional numbers and are associated with the microstructure of the considered material. In (4.18), $P_l = (\partial P/\partial Z)^{-1}$ is the gradient of the pressure which is inverted. The conditions at the considered boundary after the application of the transformations in (4.15) becomes:

$$\begin{cases}
\textbf{At Top}: u = -\alpha\frac{du}{dY}, \quad H = \omega_1 = \omega_2 = 0, \quad \forall \ (X,Y) \in T \\
\text{where} \quad T := \{(X, 0.5) : -0.5 \le X \le 0.5\} \\
\textbf{At Right and Left of the Cavity}: u = H = \omega_1 = \omega_2 = 0, \\
\quad \forall \ (X,Y) \in \mathbb{R}t \quad \text{and} \quad \forall \ (X,Y) \in L \\
\quad \text{where} \quad \mathbb{R}t := \{(0.5, Y) : -0.5 \le Y \le 0.5\} \quad \text{and} \\
\quad L := \{(-0.5, Y) : -0.5 \le Y \le 0.5\} \\
\textbf{At Bottom of the Cavity}: u = \alpha\frac{du}{dY}, \quad H = \omega_1 = \omega_2 = 0, \quad \forall \ (X,Y) \in Bt \\
\text{where} \quad Bt := \{(X, -0.5) : -0.5 \le X \le 0.5\}
\end{cases} \tag{4.22}$$

4.2 Weak Formulation

The weak formulation of the five-field problems in equations (4.16-4.22) is now calculated: Weak form of equation(4.16)

$$\frac{\partial u}{\partial X} + \frac{h}{R_m}\left(\frac{\partial^2 H}{\partial X^2} + \frac{\partial^2 H}{\partial Y^2}\right) + \frac{h_\tau}{R_m}\left[H\left(\frac{\partial^2 \omega_1}{\partial x^2} + \frac{\partial^2 \omega_1}{\partial y^2}\right) + 2\left(\frac{\partial H}{\partial X}\frac{\partial \omega_1}{\partial X} + \frac{\partial \omega_1}{\partial Y}\frac{\partial \omega_1}{\partial Y}\right)\right.$$
$$\left. + \omega_1\left(\frac{\partial^2 H}{\partial X^2} + \frac{\partial^2 H}{\partial Y^2}\right) - \left(\frac{\partial^2 \omega_2}{\partial X^2} + \frac{\partial^2 \omega_2}{\partial Y^2}\right)\right] = 0. \tag{4.23}$$

Multiply above equation by weight function $\tilde{H}$ and integrate over the domian Ω.

$$\int_\Omega \tilde{H}\cdot\Bigg[\frac{\partial u}{\partial X}+\frac{h}{R_m}\left(\frac{\partial^2 H}{\partial X^2}+\frac{\partial^2 H}{\partial Y^2}\right)+\frac{h_\tau}{R_m}\Bigg\{H\left(\frac{\partial^2\omega_1}{\partial x^2}+\frac{\partial^2\omega_1}{\partial y^2}\right) +2\left(\frac{\partial H}{\partial X}\frac{\partial \omega_1}{\partial X}+\frac{\partial \omega_1}{\partial Y}\frac{\partial \omega_1}{\partial Y}\right)+\omega_1\left(\frac{\partial^2 H}{\partial X^2}+\frac{\partial^2 H}{\partial Y^2}\right) -\left(\frac{\partial^2\omega_2}{\partial X^2}+\frac{\partial^2\omega_2}{\partial Y^2}\right)\Bigg\}\Bigg]d\Omega=0, \tag{4.24}$$

$$\int_\Omega \tilde{H}\frac{\partial u}{\partial X}d\Omega-\frac{h}{R_m}\int_\Omega\left(\frac{\partial H}{\partial X}\frac{\partial \tilde{H}}{\partial X}+\frac{\partial H}{\partial Y}\frac{\partial \tilde{H}}{\partial Y}\right)d\Omega + \frac{h_\tau}{R_m}\Bigg[-\Bigg(\int_\Omega \frac{\partial H}{\partial X}\frac{\partial \omega_1}{\partial X}\tilde{H}d\Omega+\int_\Omega H\frac{\partial \omega_1}{\partial X}\frac{\partial \tilde{H}}{\partial X}d\Omega+\int_\Omega \frac{\partial H}{\partial Y}\frac{\partial \omega_1}{\partial Y}\tilde{H}d\Omega + \int_\Omega H\frac{\partial \omega_1}{\partial Y}\frac{\partial \tilde{H}}{\partial Y}d\Omega\Bigg)+2\int_\Omega\left(\frac{\partial H}{\partial X}\frac{\partial \omega_1}{\partial X}+\frac{\partial \omega_1}{\partial Y}\frac{\partial H}{\partial Y}\right)\cdot\tilde{H}d\Omega + \int_\Omega \frac{\partial \omega_2}{\partial X}\frac{\partial \tilde{H}}{\partial X}d\Omega+\int_\Omega \frac{\partial \omega_2}{\partial Y}\frac{\partial \tilde{H}}{\partial Y}d\Omega-\Bigg\{\frac{\partial \omega_1}{\partial X}\frac{\partial H}{\partial X}\tilde{H}d\Omega + \int_\Omega \omega_1\frac{\partial H}{\partial X}\frac{\partial \tilde{H}}{\partial X}d\Omega+\frac{\partial \omega_1}{\partial Y}\frac{\partial H}{\partial Y}\tilde{H}d\Omega+\int_\Omega \omega_1\frac{\partial H}{\partial Y}\frac{\partial \tilde{H}}{\partial Y}d\Omega\Bigg\}\Bigg]=0, \quad \forall\ \tilde{H}\in H_h. \tag{4.25}$$

Weak form of equation(4.17)

$$R_eP_l+\left(\frac{1}{1-N}\right)\left(\frac{\partial^2 u}{\partial X^2}+\frac{\partial^2 u}{\partial Y^2}\right)+\left(\frac{1}{1-N}\right)\left(\frac{\partial \omega_2}{\partial X}-\frac{\partial \omega_1}{\partial Y}\right)+\xi h\left(\frac{\partial H}{\partial X}\right) +\xi h_\tau\left(H\frac{\partial \omega_1}{\partial X}+\omega_1\frac{\partial H}{\partial X}-\frac{\partial \omega_2}{\partial X}\right)=0. \tag{4.26}$$

Multiply above equation by weight function $\tilde{u}$ and integrate over the domain Ω.

$$\int_\Omega \tilde{u}\cdot\Bigg[R_eP_l+\left(\frac{1}{1-N}\right)\left(\frac{\partial^2 u}{\partial X^2}+\frac{\partial^2 u}{\partial Y^2}\right)+\left(\frac{1}{1-N}\right)\left(\frac{\partial \omega_2}{\partial X}-\frac{\partial \omega_1}{\partial Y}\right)+\xi h\left(\frac{\partial H}{\partial X}\right) +\xi h_\tau\left(H\frac{\partial \omega_1}{\partial X}+\omega_1\frac{\partial H}{\partial X}-\frac{\partial \omega_2}{\partial X}\right)\Bigg]d\Omega=0, \tag{4.27}$$

$$\Rightarrow \int_\Omega R_e P_l \cdot \tilde{u} d\Omega - \left(\frac{1}{1-N}\right)\int_\Omega \left(\frac{\partial u}{\partial X}\frac{\partial \tilde{u}}{\partial X} + \frac{\partial u}{\partial Y}\frac{\partial \tilde{u}}{\partial Y}\right) d\Omega + \left(\frac{1}{1-N}\right)\int_\Omega \left(\frac{\partial \omega_2}{\partial X} + \frac{\partial \omega_1}{\partial Y}\right)\cdot \tilde{u} d\Omega + \xi\left[h\int_\Omega \frac{\partial H}{\partial X}\tilde{H} d\Omega + h_\tau \int_\Omega \left(H\frac{\partial \omega_1}{\partial X} + \omega_1 \frac{\partial H}{\partial X} - \frac{\partial \omega_2}{\partial X}\right)\cdot \tilde{H} d\Omega\right] = 0, \quad \forall \;\; \tilde{u} \in U_h. \tag{4.28}$$

Weak form of equation (4.18)

$$\omega_1 - \frac{1}{2}\frac{\partial u}{\partial Y} - \left(\frac{2-N}{2m^2}\right)\frac{\partial^2 \omega_1}{\partial Y^2} - \frac{1}{l^2}\frac{\partial^2 \omega_1}{\partial X^2} - \left(\frac{2m^2 - l^2(2-N)}{2m^2 l^2}\right)\frac{\partial^2 \omega_2}{\partial x \partial y} - \frac{\alpha_1}{2}h_\tau\left(\frac{2-N}{m^2}\right)\omega_2 H = 0, \tag{4.29}$$

Multiply above equation by weight function $\tilde{\omega_1}$ and integrate over the domain Ω.

$$\int_\Omega \tilde{\omega_1}\cdot\left[\omega 1 - \frac{1}{2}\frac{\partial u}{\partial Y} - \left(\frac{2-N}{2m^2}\right)\frac{\partial^2 \omega_1}{\partial Y^2} - \frac{1}{l^2}\frac{\partial^2 \omega_1}{\partial X^2} - \left(\frac{2m^2 - l^2(2-N)}{2m^2 l^2}\right)\frac{\partial^2 \omega_2}{\partial x \partial y} - \frac{\alpha_1}{2}h_\tau\left(\frac{2-N}{m^2}\right)\omega_2 H\right] d\Omega = 0, \tag{4.30}$$

$$\Rightarrow -\frac{1}{2}\int_\Omega \frac{\partial u}{\partial Y}\cdot \tilde{\omega_1} d\Omega + \int_\Omega \omega_1 \cdot \tilde{\omega_1} d\Omega - \left(\frac{2-N}{2m^2}\right)\int_\Omega \frac{\partial \omega_1}{\partial Y}\cdot\frac{\partial \tilde{\omega_1}}{\partial Y} d\Omega + \left(\frac{1}{l^2}\right)\int_\Omega \frac{\partial \omega_2}{\partial X}\cdot\frac{\partial \tilde{\omega_1}}{\partial X} d\Omega + \left(\frac{2m^2 - l^2(2-N)}{2m^2 l^2}\right)\int_\Omega \frac{\partial \omega_2}{\partial Y}\cdot\frac{\partial \tilde{\omega_1}}{\partial X} d\Omega - \frac{\alpha_1}{2}h_\tau\left(\frac{2-N}{m^2}\right)\int_\Omega \omega_2 H\cdot\tilde{\omega_1} d\Omega = 0, \quad \forall \;\; \tilde{\omega_1} \in W_h. \tag{4.31}$$

weak form of equation (4.19)

$$\omega_2 + \frac{1}{2}\frac{\partial u}{\partial x} - \left(\frac{2-N}{2m^2}\right)\frac{\partial^2 \omega_2}{\partial x^2} - \frac{1}{l^2}\frac{\partial^2 \omega_2}{\partial y^2} - \left(\frac{2m^2 - l^2(2-N)}{2m^2 l^2}\right)\frac{\partial^2 \omega_1}{\partial x \partial y} - \frac{\alpha_1}{2}h_\tau\left(\frac{2-N}{m^2}\right)\omega_2 H = 0. \tag{4.32}$$

Multiply above equation by weight function $\tilde{\omega_2}$ and integrate over the domain Ω.

$$\begin{aligned}\int_\Omega \tilde{\omega_2}\cdot\Bigg[\omega_2 &+ \frac{1}{2}\frac{\partial u}{\partial x}\\ &-\left(\frac{2-N}{2m^2}\right)\frac{\partial^2\omega_2}{\partial x^2}\\ &-\frac{1}{l^2}\frac{\partial^2\omega_2}{\partial y^2}\\ &-\left(\frac{2m^2-l^2(2-N)}{2m^2l^2}\right)\frac{\partial^2\omega_1}{\partial x\partial y}\\ &-\frac{\alpha_1}{2}h_\tau\left(\frac{2-N}{m^2}\right)\omega_2 H\Bigg]d\Omega=0,\end{aligned} \tag{4.33}$$

$$\begin{aligned}\Rightarrow \frac{1}{2}\int_\Omega \frac{\partial U}{\partial X}\tilde{\omega_2}d\Omega + \int_\Omega \omega_2\tilde{\omega_2}d\Omega &+ \left(\frac{2-N}{2m^2}\right)\int_\Omega \frac{\partial \omega_2}{\partial X}\frac{\partial \omega_2}{\partial X}d\Omega\\ &+\left(\frac{1}{l^2}\right)\int_\Omega \frac{\partial\omega_2}{\partial Y}\cdot\frac{\partial\tilde{\omega_2}}{\partial Y}d\Omega\\ &+\left(\frac{2m^2-l^2(2-N)}{2m^2l^2}\right)\int_\Omega\frac{\partial\omega_1}{\partial Y}\cdot\frac{\partial\tilde{\omega_2}}{\partial X}d\Omega\\ &-\frac{\alpha_1}{2}h_\tau\left(\frac{2-N}{m^2}\right)\int_\Omega \omega_2 H\tilde{\omega_2}d\Omega=0, \qquad \forall\ \tilde{w_2}\in W_h.\end{aligned} \tag{4.34}$$

Weak form of equation (4.20)

$$\begin{aligned}&\left(\frac{\partial^2\theta}{\partial X^2}+\frac{\partial^2\theta}{\partial Y^2}\right)+Br\Bigg[\left(\frac{1}{1-N}\right)^2\left(\left(\frac{\partial u}{\partial X}\right)^2+\left(\frac{\partial u}{\partial Y}\right)^2\right)\\ &+\left(\frac{2N}{1-N}\right)\left(\omega_1^2+\omega_2^2-\omega_1\frac{\partial v}{\partial Y}+\omega_2\frac{\partial v}{\partial X}\right)\\ &+A\left(\frac{\partial\omega_1}{\partial X}+\frac{\partial\omega_2}{\partial Y}\right)^2+\left(\frac{N(2-N)}{m^2(1-N)}\right)\Bigg\{\left(\frac{\partial\omega_1}{\partial X}\right)^2+\left(\frac{\partial\omega_1}{\partial Y}\right)^2\\ &+\left(\frac{\partial\omega_2}{\partial X}\right)^2+\left(\frac{\partial\omega_2}{\partial Y}\right)^2+C\left\{\left(\frac{\partial\omega_1}{\partial X}\right)^2+\left(\frac{\partial\omega_2}{\partial Y}\right)^2+2\left(\frac{\partial\omega_1}{\partial Y}\frac{\partial\omega_1}{\partial X}\right)\right\}\Bigg\}\Bigg]\\ &+\frac{hM_p}{R_m^2}\left(\mu_0+\frac{M_0}{H}\right)\left(\frac{\partial^2 H}{\partial X^2}+\frac{\partial^2 H}{\partial Y^2}\right)+\frac{h_\tau M_p}{R_m^2}\Bigg[H\left(\frac{\partial^2\omega_1}{\partial X^2}+\frac{\partial^2\omega_1}{\partial Y^2}\right)\\ &+2\left(\frac{\partial H}{\partial X}\frac{\partial\omega_1}{\partial X}+\frac{\partial H}{\partial Y}\frac{\partial\omega_2}{\partial Y}\right)+\omega_1\left(\frac{\partial^2 H}{\partial X^2}+\frac{\partial^2 H}{\partial Y^2}\right)-\left(\frac{\partial^2\omega_1}{\partial X^2}+\frac{\partial^2\omega_2}{\partial Y^2}\right)\Bigg]=0.\end{aligned} \tag{4.35}$$

Multiply above equation by weight function $\tilde{\theta}$ and integrate over the domain Ω.

$$
\begin{aligned}
&\int_{\Omega} \tilde{\theta} \cdot \left(\frac{\partial^2 \theta}{\partial X^2} + \frac{\partial^2 \theta}{\partial Y^2} \right) d\Omega + \int_{\Omega} \tilde{\theta} \cdot Br \Bigg[\left(\frac{1}{1-N} \right)^2 \left(\left(\frac{\partial u}{\partial X} \right)^2 + \left(\frac{\partial u}{\partial Y} \right)^2 \right) \\
&\quad + \left(\frac{2N}{1-N} \right) \left(\omega_1^2 + \omega_2^2 - \omega_1 \frac{\partial v}{\partial Y} + \omega_2 \frac{\partial v}{\partial X} \right) + A \left(\frac{\partial \omega_1}{\partial X} + \frac{\partial \omega_2}{\partial Y} \right)^2 \\
&\quad + \left(\frac{N(2-N)}{m^2(1-N)} \right) \left\{ \left(\frac{\partial \omega_1}{\partial X} \right)^2 + \left(\frac{\partial \omega_1}{\partial Y} \right)^2 + \left(\frac{\partial \omega_2}{\partial X} \right)^2 + \left(\frac{\partial \omega_2}{\partial Y} \right)^2 \right\} \\
&\quad + C \left\{ \left(\frac{\partial \omega_1}{\partial X} \right)^2 + \left(\frac{\partial \omega_2}{\partial Y} \right)^2 + 2 \left(\frac{\partial \omega_1}{\partial Y} \frac{\partial \omega_1}{\partial X} \right) \right\} \Bigg] d\Omega \\
&\quad + \int_{\Omega} \tilde{\theta} \cdot \frac{h M_p}{R_m^2} \left(\mu_0 + \frac{M_0}{H} \right) \left(\frac{\partial^2 H}{\partial X^2} + \frac{\partial^2 H}{\partial Y^2} \right) d\Omega \\
&\quad + \int_{\Omega} \tilde{\theta} \cdot \frac{h_\tau M_p}{R_m^2} \Bigg[H \left(\frac{\partial^2 \omega_1}{\partial X^2} + \frac{\partial^2 \omega_1}{\partial Y^2} \right) + 2 \left(\frac{\partial H}{\partial X} \frac{\partial \omega_1}{\partial X} + \frac{\partial H}{\partial Y} \frac{\partial \omega_2}{\partial Y} \right) \\
&\quad + \omega_1 \left(\frac{\partial^2 H}{\partial X^2} + \frac{\partial^2 H}{\partial Y^2} \right) - \left(\frac{\partial^2 \omega_1}{\partial X^2} + \frac{\partial^2 \omega_2}{\partial Y^2} \right) \Bigg] d\Omega = 0. \qquad (4.36)
\end{aligned}
$$

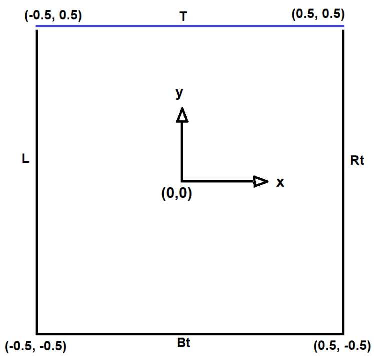

(a)

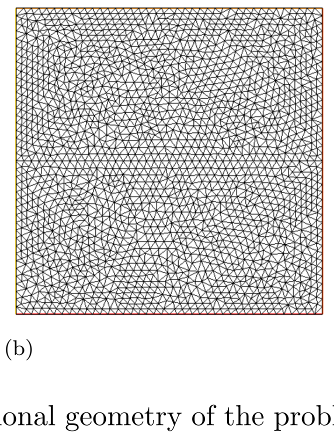

(b)

FIGURE 4.1: (a) Computational geometry of the problem, (b) Descretized mesh of the computational domain.

$$
\begin{aligned}
&\left(\frac{\partial\theta}{\partial X}\frac{\partial\tilde{\theta}}{\partial X}+\frac{\partial\theta}{\partial Y}\frac{\partial\tilde{\theta}}{\partial Y}\right)\\
&+Br\left[\left(\frac{1}{1-N}\right)^2\left(\frac{\partial u}{\partial X}\frac{\partial u}{\partial X}+\frac{\partial u}{\partial Y}\frac{\partial u}{\partial Y}\right)\cdot\tilde{\theta}\right.\\
&+\left(\frac{2N}{1-N}\right)\left\{\omega_1\left(\omega_1-\frac{\partial u}{\partial Y}\right)+\omega_2\left(\omega_2+\frac{\partial u}{\partial X}\right)\right\}\cdot\tilde{\theta}\\
&+A\left(\frac{\partial\omega_1}{\partial X}+\frac{\partial\omega_2}{\partial Y}\right)^2\cdot\tilde{\theta}\\
&+\left(\frac{N(2-N)}{m^2(1-N)}\right)\left(\frac{\partial\omega_1}{\partial X}^2+\frac{\partial\omega_1}{\partial Y}^2+\frac{\partial\omega_2}{\partial X}^2+\frac{\partial\omega_2}{\partial Y}^2\right)\cdot\tilde{\theta}\\
&\left.+C\left\{\frac{\partial\omega_1}{\partial X}^2+\frac{\partial\omega_2}{\partial X}\frac{\partial\omega_2}{\partial Y}+2\left(\frac{\partial\omega_1}{\partial Y}\frac{\partial\omega_1}{\partial X}\right)\right\}\cdot\tilde{\theta}\right]\\
&-\frac{Ha^2B_r}{R_m^2B_0^2}\left(\mu_0+\frac{M_0}{\bar{H}}\right)\int_\Omega\left(\frac{\partial H}{\partial X}\frac{\partial\tilde{\theta}}{\partial X}+\frac{\partial H}{\partial Y}\frac{\partial\tilde{\theta}}{\partial Y}\right)d\Omega\\
&+\frac{h_\tau}{R_m}B_0\sigma\mu_0a^2\left[-\left(\int_\Omega\frac{\partial H}{\partial X}\frac{\partial\omega_1}{\partial X}\tilde{\theta}d\Omega+\int_\Omega H\frac{\partial\omega_1}{\partial X}\frac{\partial\tilde{\theta}}{\partial X}d\Omega\right.\right.\\
&\left.+\int_\Omega\frac{\partial H}{\partial Y}\frac{\partial\omega_1}{\partial Y}\tilde{\theta}d\Omega+\int_\Omega H\frac{\partial\omega_1}{\partial Y}\frac{\partial\tilde{\theta}}{\partial Y}d\Omega\right)\\
&+2\int_\Omega\left(\frac{\partial H}{\partial X}\frac{\partial\omega_1}{\partial X}+\frac{\partial H}{\partial Y}\frac{\partial\omega_2}{\partial Y}\right)\cdot\tilde{\theta}d\Omega\\
&-\left(\int_\Omega\frac{\partial\omega_1}{\partial X}\frac{\partial H}{\partial X}\tilde{\theta}d\Omega+\int_\Omega\omega_1\frac{\partial H}{\partial X}\frac{\partial\tilde{\theta}}{\partial X}d\Omega\right.\\
&\left.+\int_\Omega\frac{\partial\omega_1}{\partial Y}\frac{\partial H}{\partial Y}\tilde{\theta}d\Omega+\int_\Omega\omega_1\frac{\partial H}{\partial Y}\frac{\partial\tilde{\theta}}{\partial Y}d\Omega\right)\\
&\left.+\int_\Omega\left(\frac{\partial\omega_1}{\partial X}\frac{\partial\tilde{\theta}}{\partial X}+\frac{\partial\omega_2}{\partial Y}\frac{\partial\tilde{\theta}}{\partial Y}\right)d\Omega\right]=0,\quad\forall\ \tilde{\theta}\in\Theta_h.
\end{aligned}
\tag{4.37}
$$

Chapter 5

Results and Discussion

In this chapter, we present results computed using the finite element method. The results are calculated for varying different material parameters and are discussed in detail. The computational domain is discretized into number of finite elements with number of vertices. FreeFEM++ code is developed to calculate the solution numerically over the discretized mesh for different material's parameter setting. The variables of interest in this study are the translational velocity of the fluid particles, micromagnetorotaional velocities, and the temperature field variable. These velocities and temperature fields are plotted in different test cases where different material parameter settings are taken into account. In Figure 5.1 the effect of α_1 is analyzed on the isotherm plots in the presence and absence of micromagnetorotation (MMR). The physical parameters used in the computations of these isotherms are taken to be $Re = 4$, $Br = m = A = Bi = Pl = 1$, $En = 0.4$, $C = \alpha = 0.1$, $Rm = 10$, $l = 0.5$, and $Mp = \xi = 0$. Whenever the effect of MMR is considered the material parameters h and h_τ are assumed of unit value and whenever the case without MMR is taken these material parameters are assumed a value equals to zero. The subfigures in the left column of Figure 5.1 are isotherm plots in the absence of MMR effect whereas the right column subfigures are in the presence of MMR effect. It is observed that when α_1 is zero there is no difference in the temperature field within the medium in the presence and absence of MMR. That implies that when $\alpha_1 = 0$ the MMR do not effect the temperature in the medium. However, when the parameter α_1 gets a non-zero value then the presence of MMR influence the temperature within the medium. It is also observed that the temperature in the presence of MMR gets larger values as compared to that in the absence of MMR effect with the considered medium. Moreover, with increasing value of the material parameter α_1 the temperature in the medium in increasing in magnitude more profoundly in the presence of MMR effect within the medium in comparsion to the case of without MMR consideration.

In the Figure 5.2, Isotherms are plotted for varying values of the physical parameter M_p in the presence and absence of MMR effects. The other parameters used in these simulations are: $Re = 4$, $Br = m = A = Bi = Pl = 1$, $En = 0.4$, $C = \alpha = 0.1$, $Rm = 10$, $l = 0.5$, and $\alpha_1 = \xi = 0$. In the left column the sub-figures are computed for varying M_p values in the absence of MMR effects.

While in the right column the sub-figures are computed for varying M_p values in the presence of MMR effects. The material parameters h and h_τ takes the zero values in the absence of MMR effects. While in the presence of MMR effects these parameters are assume a unit value.In both situations, it is found that the medium's temperature rises as the value of Mp increases.

That is in the absence and present of MMR effects the temperature get increased with increasing value of the parameter M_p.However, it is observed that the presence of MMR effects perturbs the medium's isotherms for nonzero values of the parameter M_p. This is highly due to the magnetization effect which leads to the unstability in of the isotherms in the medium for larger values of M_p. However, in the absence of MMR this unstability do not arises as the micromagnetorotaiton effects are absent. In Figure 5.3, microrotation velocity field is plotted for varying values of the parameter l. These microrotation velocities are calculated in the presence of MMR. The parameters used in these computations are taken to be $Re = 4$, $Br = m = A = Bi = Pl = 1$, $En = 0.4$, $C = \alpha = 0.1$, $Rm = 10$, $\alpha_1 = \xi = Mp = 0.$, $h_\tau = 1.0$, and $h = 100$. It is seen that the microrotation velocities within the medium are decreasing with increasing values of the parameter l. In the Figure 5.4, the effect of parameter α is shown on the distribution of translational velocities within the cavity. These velocities are computed with the consideration of the MMR effect.

The material parameters used in these numerical simulations are $Re = 4$, $Br = m = A = Bi = Pl = 1$, $En = 0.4$, $C = 0.1$, $Rm = 10$, $\alpha_1 = \xi = Mp = 0$, $h_\tau = 1.0$ and

$h = 1$.

It is seen that the translational velocity contours over the domain vary with varying values of the physical parameter α. With increasing values of the parameter α the maximum magnitude of the translational velocity is increasing.

Initially for $\alpha = 0$ there is one maximum of the velocity function within the domain but with the increasing values of α the velocity distribution function within the domain changes and two maxima arises within the domain of the cavity.

Moreover, increasing the value of parameter α leads to a saddle type velocity distribution function within the cavity domain. In Figure 5.5, the temperature plots are shown for varying values of the physical parameter Bi. These isotherms are calculated with the consideration of MMR effect. The parameters used in these simulations takes the the values as $Re = 4$, $Br = m = A = Bi = Pl = 1$, $En = 0.4$, $C = 0.1$, $Rm = 10$, $\alpha_1 = \xi = Mp = 0$, $h_\tau = 1.0$, and $h = 1$. The physical parameter Bi is varied between zero and one. It is seen that in the presence of MMR the temperature within the medium gets increased with increasing values of the parameter Bi.

In Figure 5.6, the effect of parameter En are depicted on the translational velocity of the fluid particles within the cavity in the presence of MMR.

The parameters used in these computations are $Re = 4$, $Br = m = A = Bi = Pl = 1$, $En = 0.4$, $\alpha = C = 0.1$, $Rm = 0.1$, $\alpha_1 = \xi = Mp = 0$, $h_\tau = 1.0$, and $h = 1$.

It is seen that with increasing values of the parameter En the translational velocities of the fluid particles get decrease.

In Figure 5.7, the microrotational velocity of the fluid particles is depicted in the presence of MMR. The effect of parameter m is shown on the microrotation velcity within the medium. These microrotational velocities are computed with the parameter values as $Re = 4$, $Br = A = Bi = Pl = 1$, $En = 0.1$, $\alpha = C = 0.1$, $Rm = 0.1$, $\alpha_1 = \xi = Mp = 0$, $l = 10.5$, $h_\tau = 1.0$ and $h = 1$. It is observed that with increasing values of the parameter m the microrotational velocities within the medium is increased. Moreover, it is noted for smaller values of m the microrotaional velocity distribution within the medium is symmetric, however, this turns into asymmetric distribution of the microrotaional velocity with increasing values of the parameter m.

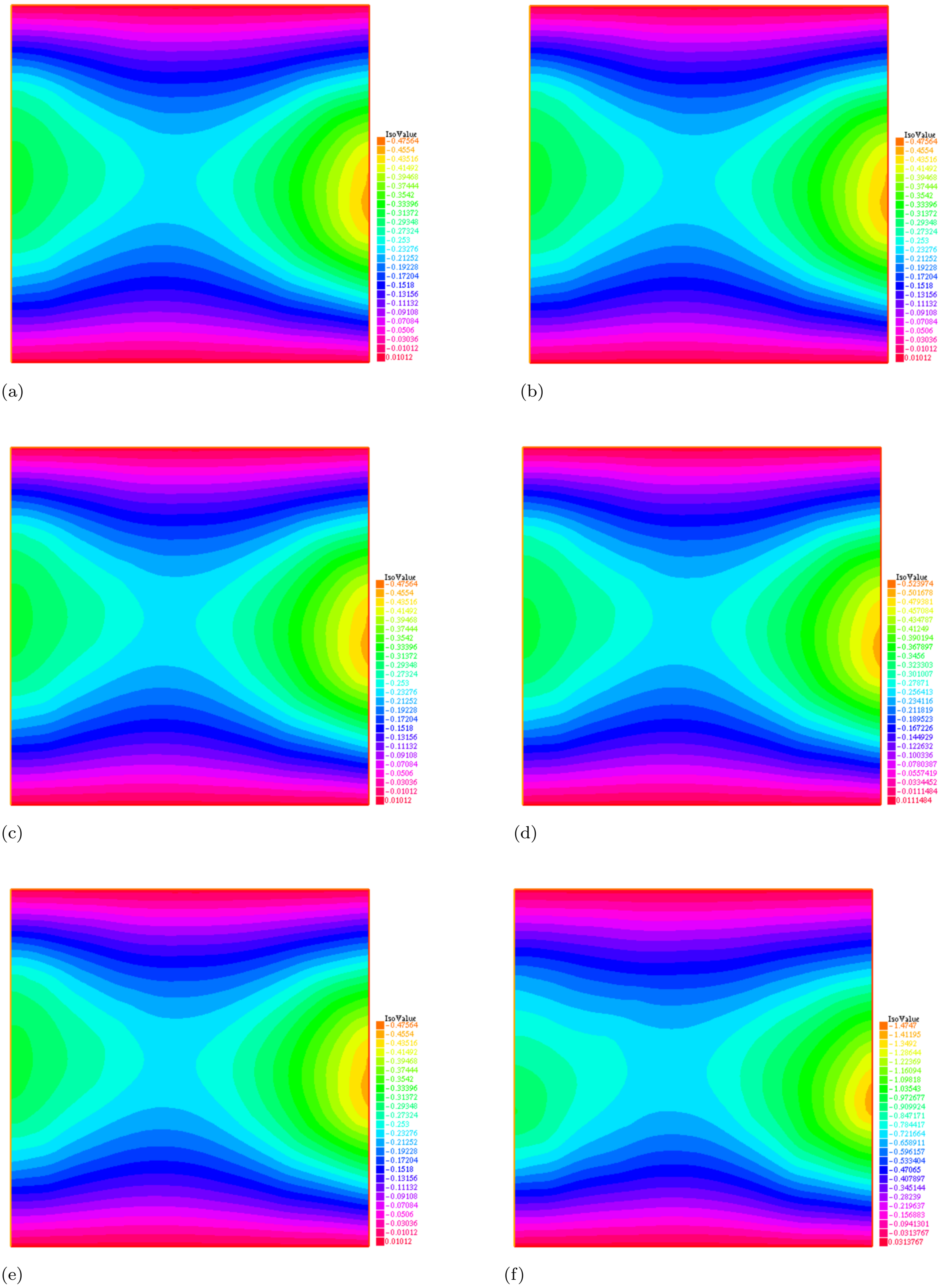

FIGURE 5.1: Temperature plots for varying values of α_1 in the presence and absence of MMR. (a) $\alpha_1 = 0$, without MMR. (b) $\alpha_1 = 0$, with MMR. (c) $\alpha_1 = 100$, without MMR. (d) $\alpha_1 = 100$, with MMR. (e) $\alpha_1 = 1000$, without MMR. (f) $\alpha_1 = 1000$, with MMR.

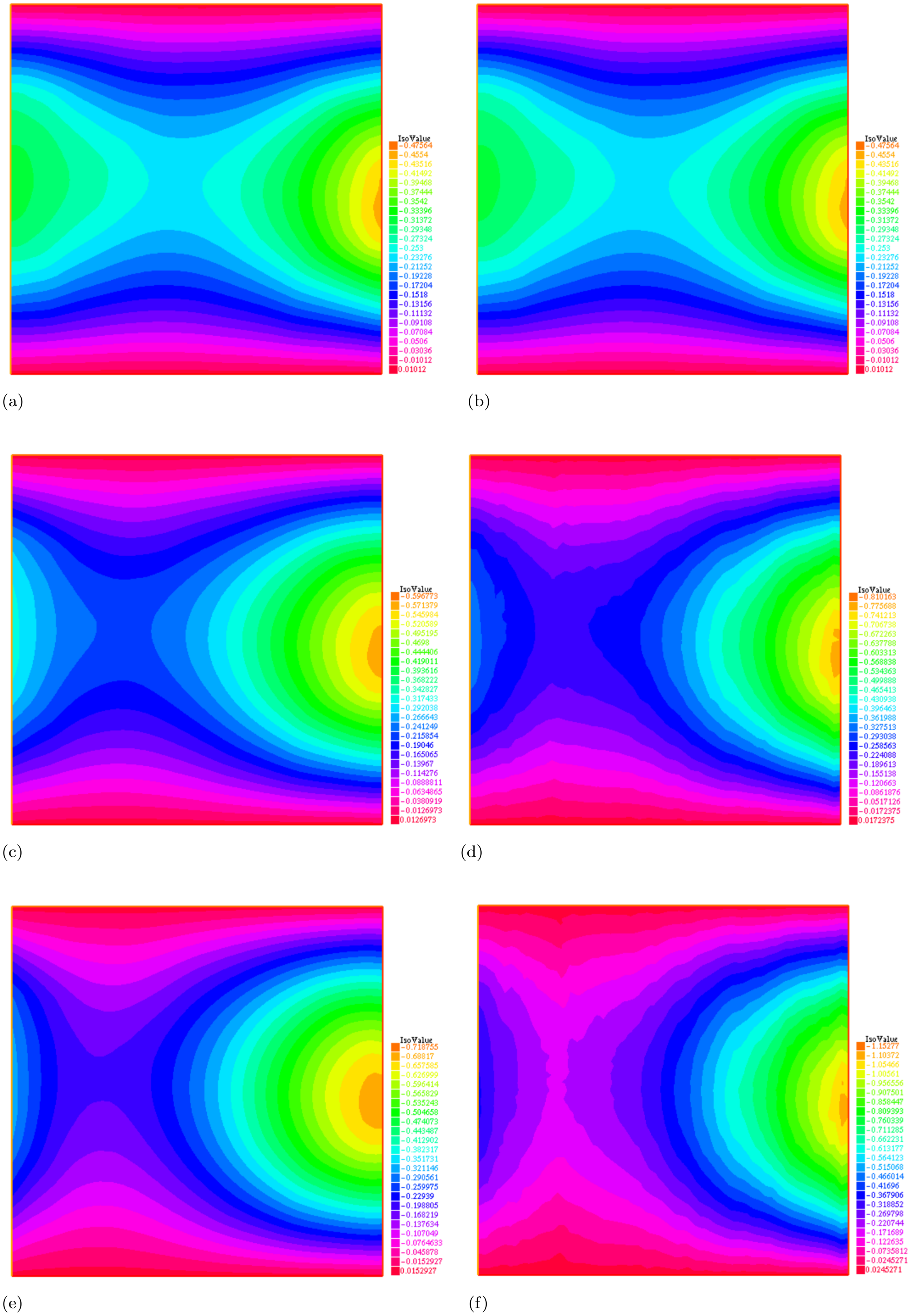

FIGURE 5.2: Effect of Mp on θ in the presence and absence of MMR. (a) $Mp = 0$, without MMR. (b) $Mp = 0$, with MMR. (c) $Mp = 50$, without MMR. (d) $Mp = 50$, with MMR. (e) $Mp = 100$, without MMR. (f) $Mp = 100$, with MMR.

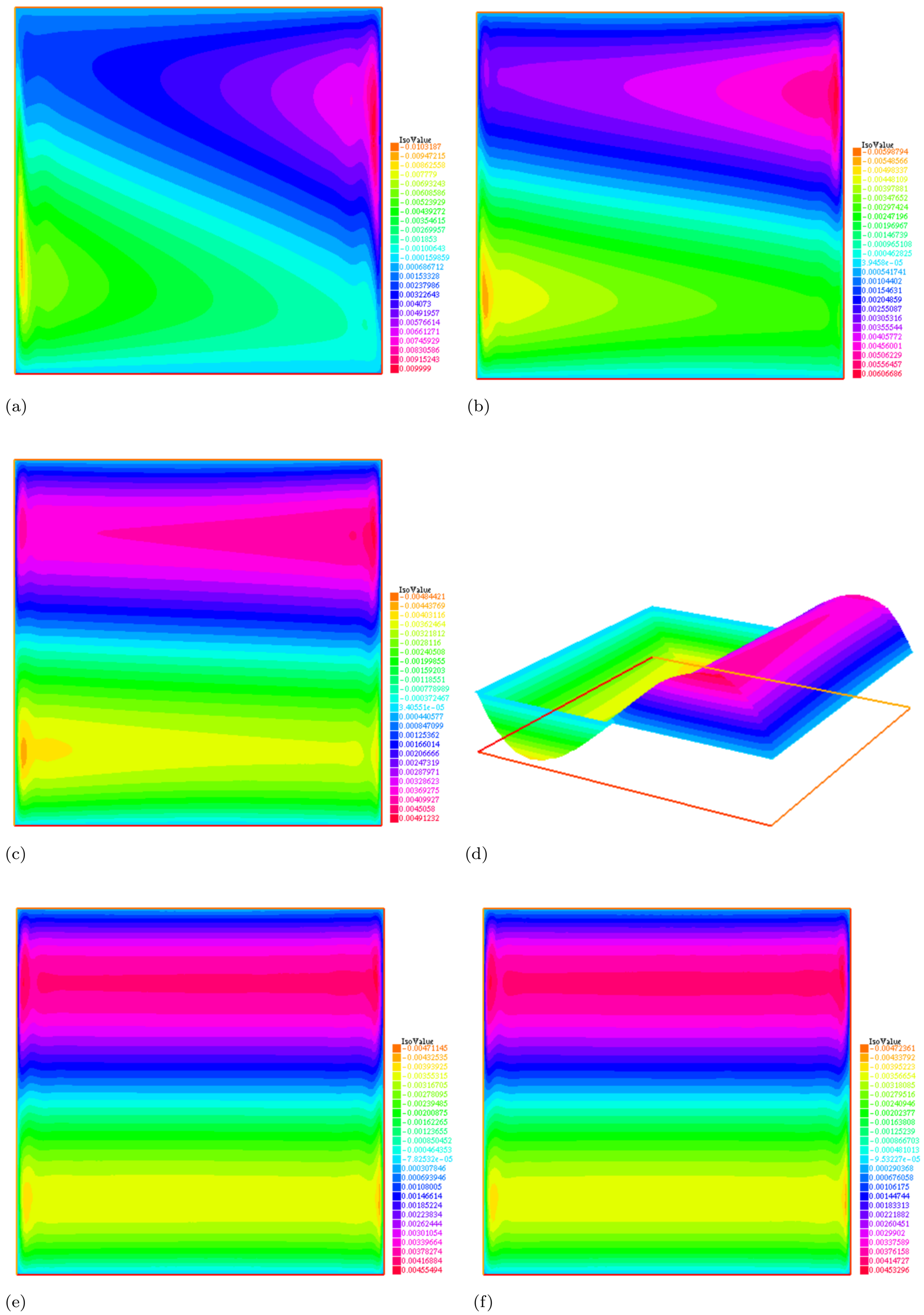

FIGURE 5.3: Effect of l on the microrotation velocity w_1 in the presence of MMR. (a) For $l = 3.5$ (b) For $l = 5.5$ (c) For $l = 10.5$ (d) For $l = 40.5$, (e) For $l = 100.5$

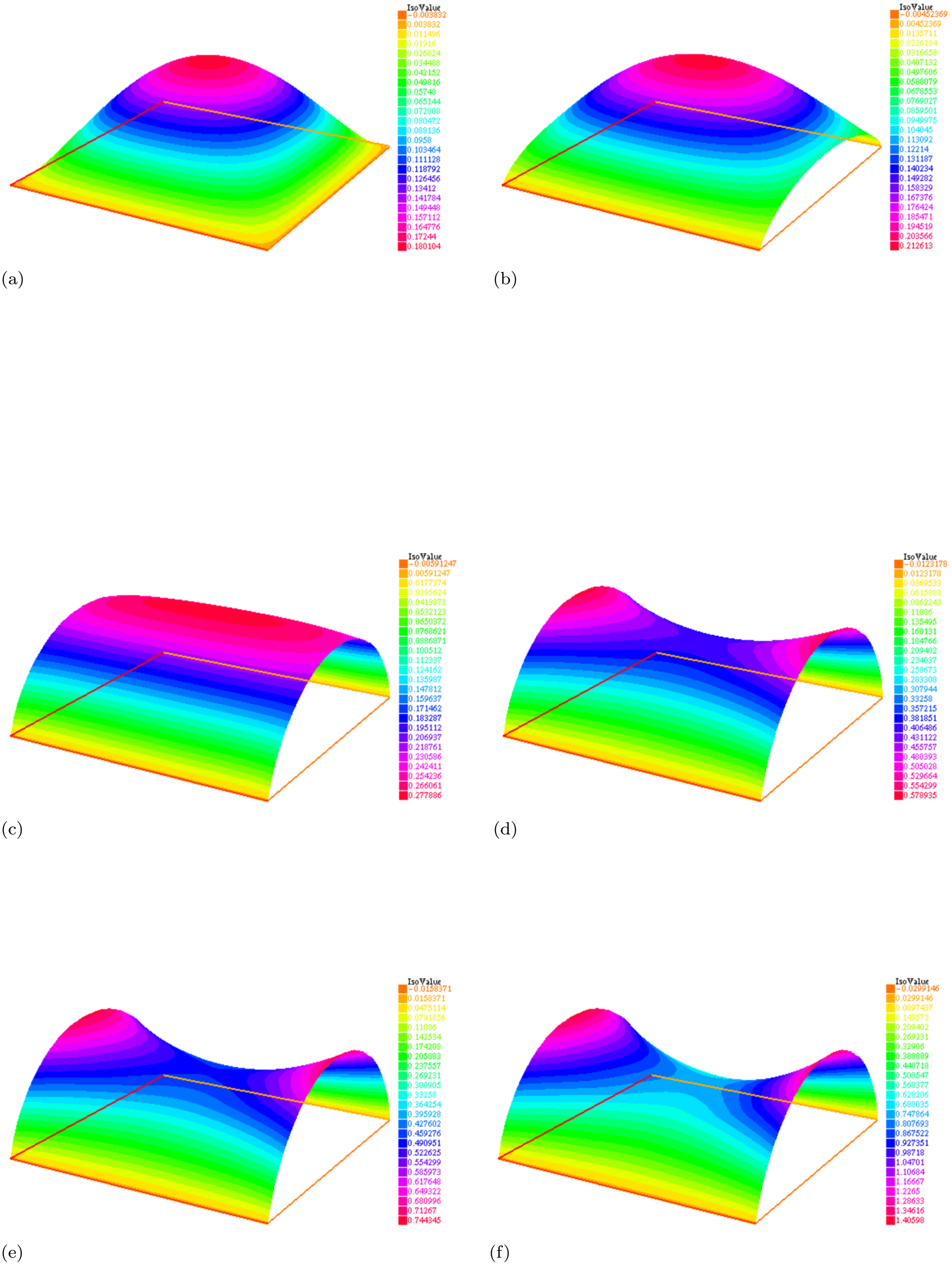

FIGURE 5.4: Effect of α on the translational velocity u in the presence of MMR. (a) For $\alpha = 0$ (b) For $\alpha = 0.1$ (c) For $\alpha = 0.3$ (d) For $\alpha = 0.7$, (e) For $\alpha = 0.9$, (f) For $\alpha = 1.7$

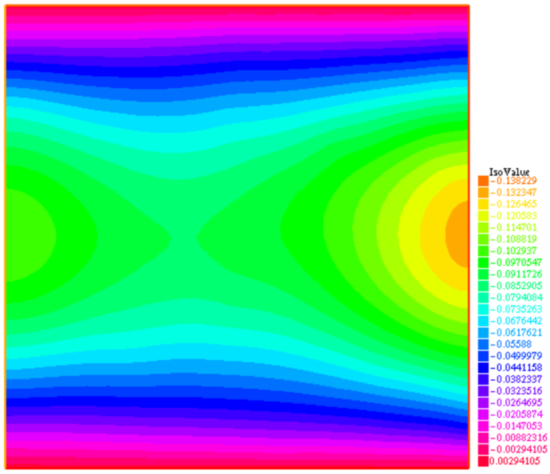

(a)

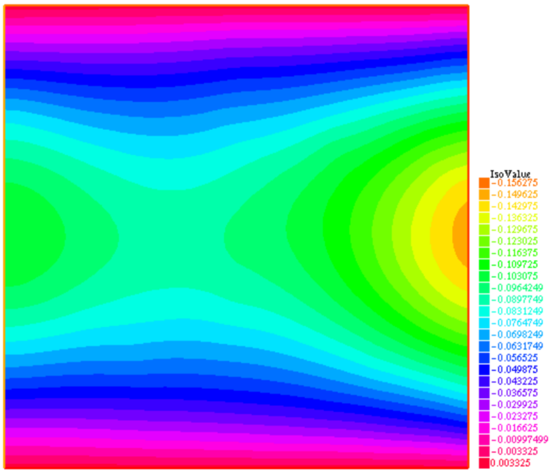

(b)

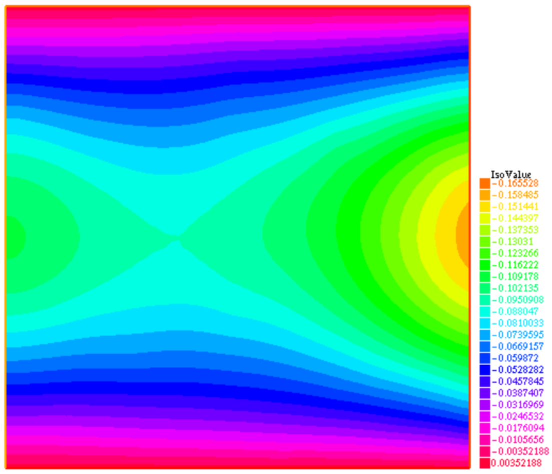

(c)

FIGURE 5.5: Effect of Bi on the temperature θ in the presence of MMR. (a) For $Bi = 0$ (b) For $Bi = 0.7$ (c) For $Bi = 1$.

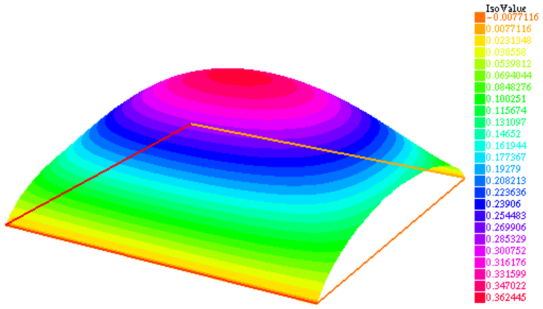

(a)

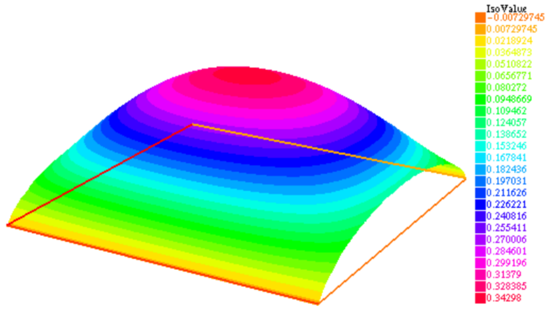

(b)

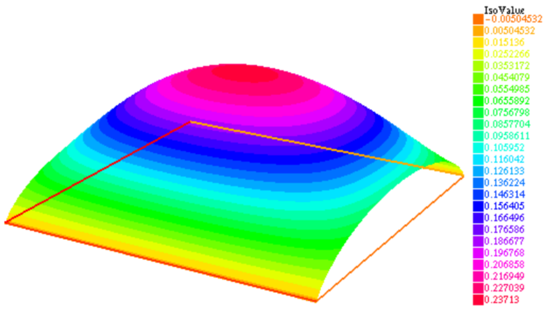

(c)

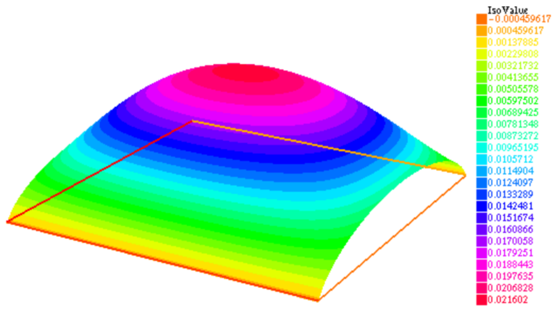

(d)

FIGURE 5.6: Effect of En on the u velocity in the presence of MMR. (a) For $En = 0$ (b) For $En = 0.04$ (c) For $En = 0.34$ (d) For $En = 0.94$

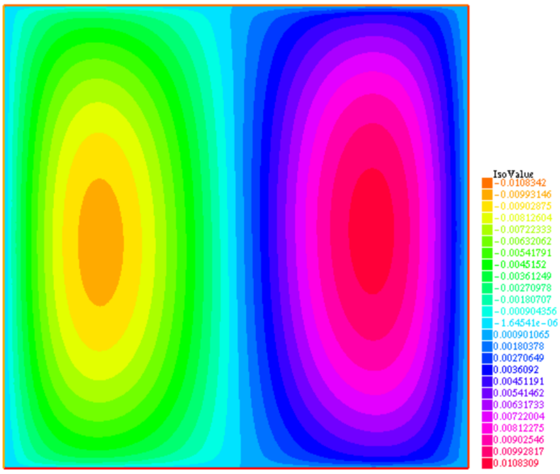

(a)

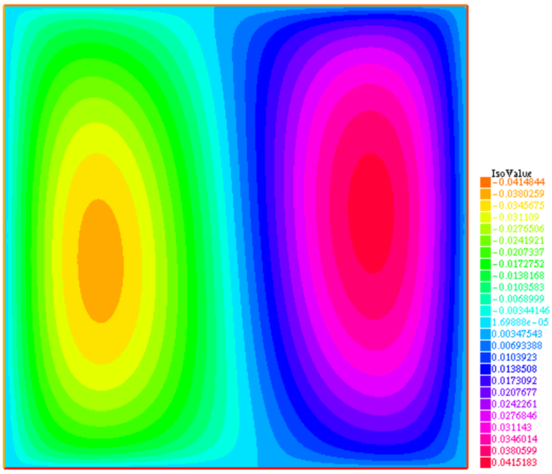

(b)

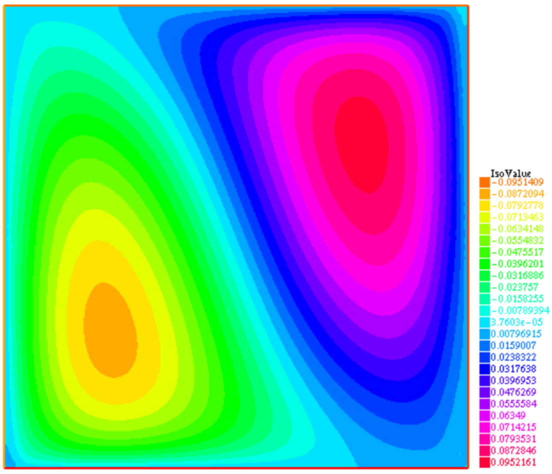

(c)

FIGURE 5.7: Effect of m on the microrotational velocity ω_2 in the presence of MMR. (a) For $m = 1$ (b) For $m = 2$ (c) For $m = 3$

Chapter 6

Conclusions and Future Directions

In this thesis, finite element analysis of a thermal flow model is presented with the consideration of micromagnetorotation (MMR) effects. To study the effect of MMR on the thermal and hydrodynamics of the considered flow system first a model presented by Khan and Isma [16] is studied. Their work is afterwards extended to include the effect of MMR. This is done so to analyze the effect of MMR on the thermal, velocity and microrotational velocity fields within the considered flow. The flow is considered in a square cavity for convenience. The geometry and the associated boundary conditions are described. The extended model governing the flow dynamics within the cavity is presented in the for of partial differential equations (PDEs). The effect of MMR is incorporated in the flow governing PDEs following the work of Khan [16]. The non-dimensional analysis of the presented PDEs model is then calculated. This non-dimensinalized system is then used to construct a weak formulation of the associated flow problem. The constructed weak formulation is used to implement in the open source code FreeFEM++ which is based on the finite element method. Numerical simulations are performed to compute the solution of the cavity flow problem under different material parameter setting. Results are computed and presented for the temperature, velocity and microrotatinal velocity field variables for varying physical parameters in the presence and absence of MMR effect. The main findings in this thesis are summarized as follows:

- It is also observed that the temperature in the presence of MMR gets larger values as compared to that in the absence of MMR effect with the considered medium.

- With increasing value of the material parameter α_1 the temperature in the medium in increasing in magnitude more profoundly in the presence of MMR effect within the medium in comparsion to the case of without MMR consideration.

- Increasing value of M_p leads to an increased temperature within the medium in the presence and absence of MMR effect. However, it is seen that for nonzero values of the parameter M_p the isotherms in the medium gets perturbed in the presence of MMR effects.

  This is highly due to the magnetization effect which leads to the unstability in of the isotherms in the medium for larger values of M_p. However, in the absence of MMR this unstability do not arises as the micromagnetorotaiton effects are absent.

- With increasing values of the parameter α the maximum magnitude of the translational velocity is increasing. Initially for $\alpha = 0$ there is one maximum of the velocity function within the domain but with the increasing values of α the velocity distribution function within the domain changes and two maxima arises within the domain of the cavity. Moreover, increasing the value of parameter α leads to a saddle type velocity distribution function within the cavity domain.

- It is seen that in the presence of MMR the temperature within the medium gets increased with increasing values of the parameter Bi.

- Increasing values of the parameter En leads to a decrease in the translational velocities of the fluid particles within the medium.

- With increasing values of the parameter m the microrotational velocities within the medium is increased. Moreover, for smaller values of m the microrotaional velocity distribution within the medium is symmetric, however, this turns into asymmetric distribution of the microrotaional velocity with increasing values of the parameter.

In future, the model presented in this thesis can be analyzed for different geometries, such as open channel flows, flows in channels with steps, and more complex geometries. Moreover, the study presented can also be extended to a three dimensional setting where the other component of the translational and microrotational velocities are considered. This will lead to analyze more realistic fluids structures in industrial applications.

Bibliography

[1] Ronald E Rosensweig. Heating magnetic fluid with alternating magnetic field. *Journal of magnetism and magnetic materials*, 252:370–374, 2002.

[2] M Sheikholeslami and D D Ganji. Magnetohydrodynamic flow in a permeable channel filled with nanofluid. *Scientia Iranica*, 21(1):203–212, 2014.

[3] Lizhi Jia, Shen Wei, and Junjie Liu. A review of optimization approaches for controlling water-cooled central cooling systems. *Building and Environment*, 203: 108100, 2021.

[4] Lizhi Jia, Shen Wei, and Junjie Liu. A review of optimization approaches for controlling water-cooled central cooling systems. *Building and Environment*, 203: 108100, 2021.

[5] Pei-Xin Qin, Han Yan, Xiao-Ning Wang, Ze-Xin Feng, Hui-Xin Guo, Xiao-Rong Zhou, Hao-Jiang Wu, Xin Zhang, Zhao-Guo-Gang Leng, Hong-Yu Chen, et al. Noncollinear spintronics and electric-field control: a review. *Rare Metals*, 39: 95–112, 2020.

[6] ZANG Xuzhong, SHI Er, FU Junping, and YU Tao. A review of magnetic field effects on flow and heat transfer in magnetic nanofluids. *Chemical Industry and Engineering Progress*, 38(12):5410, 2019.

[7] Cindi L Dennis and Robert Ivkov. Physics of heat generation using magnetic nanoparticles for hyperthermia. *International Journal of Hyperthermia*, 29(8): 715–729, 2013.

[8] Silong Zhang, Xin Li, Jingying Zuo, Jiang Qin, Kunlin Cheng, Yu Feng, and Wen Bao. Research progress on active thermal protection for hypersonic vehicles. *Progress in Aerospace Sciences*, 119:100646, 2020.

[9] William Fuller Brown Jr. Micromagnetics, domains, and resonance. *Journal of Applied Physics*, 30(4):S62–S69, 1959.

[10] Huei Chu Weng, MIN-HSING CHANG, et al. Stability of micropolar fluid flow between concentric rotating cylinders. *Journal of Fluid Mechanics*, 631:343–362, 2009.

[11] Zhaodong Ding, Yongjun Jian, Lin Wang, and Liangui Yang. Analytical investigation of electrokinetic effects of micropolar fluids in nanofluidic channels. *Physics of Fluids*, 29(8), 2017.

[12] Kyriaki-Evangelia Aslani, Lefteris Benos, Efstratios Tzirtzilakis, and Ioannis E Sarris. Micromagnetorotation of mhd micropolar flows. *Symmetry*, 12(1):148, 2020.

[13] Harmindar S Takhar, R Bhargava, RS Agrawal, and AVS Balaji. Finite element solution of micropolar fluid flow and heat transfer between two porous discs. *International journal of engineering science*, 38(17):1907–1922, 2000.

[14] M Sabeel Khan, Isma Hameed, M Asif Memon, and Ebenezer Bonyah. Computational analysis of magnetic induced micropolar flow in a rectangular channel through freefem++. *AIP Advances*, 13(4), 2023.

[15] Md Mohidul Haque. Heat and mass transfer analysis on magneto micropolar fluid flow with heat absorption in induced magnetic field. *Fluids*, 6(3):126, 2021.

[16] MS Khan and I Hameed. Freefem++ based heat transfer analysis of an electrically induced magnetic flow within the framework of micropolar continuum. *Numerical Heat Transfer, Part A: Applications*, 85(18):3110–3128, 2024.

[17] PK Pattnaik, SR Mishra, and Subhajit Panda. Response surface methodology on optimizing heat transfer rate for the free convection of micro-structured fluid through permeable shrinking surface. *The European Physical Journal Plus*, 139 (3):221, 2024.

[18] Shankar Goud Bejawada and Mahantesh M Nandeppanavar. Effect of thermal radiation on magnetohydrodynamics heat transfer micropolar fluid flow over a vertical moving porous plate. *Experimental and Computational Multiphase Flow*, 5(2):149–158, 2023.

[19] D Gupta, Lokendra Kumar, O Anwar Bég, and B Singh. Finite element analysis of mhd flow of micropolar fluid over a shrinking sheet with a convective surface boundary condition. *Journal of Engineering Thermophysics*, 27:202–220, 2018.

[20] MD Shamshuddin and WJIJoM Ibrahim. Finite element numerical technique for magneto-micropolar nanofluid flow filled with chemically reactive casson fluid between parallel plates subjected to rotatory system with electrical and hall currents. *International Journal of Modelling and Simulation*, 42(6):985–1004, 2022.

[21] Harmindar S Takhar, R Bhargava, RS Agrawal, and AVS Balaji. Finite element solution of micropolar fluid flow and heat transfer between two porous discs. *International journal of engineering science*, 38(17):1907–1922, 2000.

[22] Ian Papautsky, John Brazzle, Timothy Ameel, and A Bruno Frazier. Laminar fluid behavior in microchannels using micropolar fluid theory. *Sensors and actuators A: Physical*, 73(1-2):101–108, 1999.

[23] Achintya Kambli and Prasenjit Dey. A critical review on recent developments and applications of microchannels in the field of heat transfer and energy. *Heat and Mass Transfer*, 59(9):1707–1747, 2023.

[24] Zhenfei Feng, Zhenzhou Li, Zhenjun Hu, Yongqi Lan, Siyao Zheng, Qingyuan Zhang, Jianyang Zhou, and Jinxin Zhang. Combined influence of rectangular wire coil and twisted tape on flow and heat transfer characteristics in square mini-channels. *International Journal of Heat and Mass Transfer*, 205:123866, 2023.

[25] Milad Amiri and Dariusz Mikielewicz. Three-dimensional numerical investigation of hybrid nanofluids in chain microchannel under electrohydrodynamic actuator. *Numerical Heat Transfer, Part A: Applications*, 83(10):1146–1173, 2023.

[26] R. Sivakumar Samit Ghosh, Subharthi Sarkar and T. V. S. Sekhar. Forced convection magnetohydrodynamic flow past a circular cylinder by considering the

penetration of magnetic field inside it. *Numerical Heat Transfer, Part A: Applications*, 76(1):32–49, 2019.

[27] Heat transfer and interfacial flow physics of microgravity flow boiling in single-side-heated rectangular channel with subcooled inlet conditions – experiments onboard the international space station. *International Journal of Heat and Mass Transfer*, 207:123998, 2023. ISSN 0017-9310. doi: https://doi.org/10.1016/j.ijheatmasstransfer.2023.123998.

[28] JV Murthy, KS Sai, and NK Bahali. Steady flow of micropolar fluid in a rectangular channel under transverse magnetic field with suction. *AIP Advances*, 1(3), 2011.

[29] T. Asim Y. P. Kumar, S. Jaiswal and R. Mishra. Influence of a magnetic field on the flow of a micropolar fluid sandwiched between two newtonian fluid layers through a porous medium,. *European physical journal plus*, 2018.

[30] A. Borrelli, G. Giantesio, and M.C. Patria. Magnetoconvection of a micropolar fluid in a vertical channel. *International Journal of Heat and Mass Transfer*, 80: 614–625, 2015.

[31] Muhammad Sabeel Khan and Klaus Hackl. *Modeling of Microstructures in a Cosserat Continuum Using Relaxed Energies*, pages 103–125. Springer International Publishing, Cham, 2018.

[32] Igor V Miroshnichenko, Mikhail A Sheremet, Ioan Pop, and Anuar Ishak. Convective heat transfer of micropolar fluid in a horizontal wavy channel under the local heating. *International Journal of Mechanical Sciences*, 128:541–549, 2017.

[33] Saeed Dinarvand, M. Saber, and Milad Abulhasansari. Micropolar fluid flow and heat transfer about a spinning cone with hall current and ohmic heating. *Proceedings of the Institution of Mechanical Engineers, Part C: Journal of Mechanical Engineering Science*, 228:1900 – 1912, 2014. URL https://api.semanticscholar.org/CorpusID:123630169.

[34] H. ASADI, K. JAVAHERDEH, and S. RAMEZANI. Micropolar fluid model for blood flow through a stenosed artery. *International Journal of Applied Mechanics*, 05(04):1350043, 2013.

[35] Sabeel M Khan and H Kaneez. Numerical computation of heat transfer enhancement through cosserat hybrid nanofluids using continuous galerkin–petrov method. *The European Physical Journal Plus*, 135(2):1–19, 2020.